Journal of Cleaner Production 208 (2019) 753–777

Contents lists available at ScienceDirect

Journal of Cleaner Production

journal homepage: www.elsevier.com/locate/jclepro

The compatibility of controlled power plants with self-sustainable models using a hybrid input/output and water-energy-carbon nexus analysis for climate change adaptation

Pouya Ifaei, ChangKyoo Yoo*

Dept. of Environmental Science and Engineering, College of Engineering, Center for Environmental Studies, Kyung Hee University, Seocheon-dong 1, Giheung-gu, Yongin-Si, Gyeonggi-Do, 446-701, South Korea

ARTICLE INFO

Article history:
Received 13 June 2018
Received in revised form
26 September 2018
Accepted 13 October 2018
Available online 15 October 2018

Keywords:
Climate change adaptation
Controlled power plant
Life cycle assessment
Power and freshwater cogeneration
Renewable energy
Self-sustainability
Water-energy-carbon nexus

ABSTRACT

In the present study, a novel model-based approach is detailed for optimal design and analysis of clean and economic production technologies regardless of temporal and local restrictions. Accordingly, a dual-layer mathematical model is developed in which techno-economic and life cycle analyses are integrated in the first layer using a novel self-sustainability flowchart and the nexus between the water, energy, and carbon sectors are investigated in the second layer using an input/output analysis. A water and energy intensive system consisting of non-renewable (NRES) and renewable energy subsystems (HRES), a reverse osmosis module and a fuel cycle, is studied using the approach and the results are validated and calibrated according to the relevant literature. Four scenarios including an NRES fueled by pulverized coal (I) and natural gas (II), a hybrid NRES and HRES application (III), and a power and freshwater cogeneration system (IV) are compared from both economic and environmental viewpoints. Finally, the applicability of the controlled NRES is investigated using economic, environmental, and combined environmental-economic cost of products (CEECP) and the sensitivity of the model responses with respect to the manipulating variable is studied. The results showed that CEECP was obtained to be 164.7, 134.1, 515.2, and 134.1 $/MWh in the scenarios I, II, III, and IV, respectively. Additionally, the operational water withdrawal could be decreased by 1.7–3.2% in favor of additional 0.03–0.05% of CO_2-eq emissions by employing a controlled power plant.

© 2018 Elsevier Ltd. All rights reserved.

1. Introduction

A critical environmental situation has emerged as a consequence of rapid industrialization, population growth and resources depletion in recent decades. Hence, there has been a considerable attempt to seek both cleaner production technologies and novel management strategies to meet sustainable development plans due to recent concerns (Ifaei et al., 2017b). With respect to integrated industries, no improvement can be sustainably achieved unless the complicated interconnections between industries are appropriately understood.

The conjoint concept of the water-energy nexus involves energy-intensive water withdrawal, treatment and distribution as well as water losses in all stages of energy production (Thiede et al., 2016). The water-energy nexus was successfully targeted in the engineering systems' optimization reducing both “energy for water” and “water for energy” (Ifaei et al., 2016a; Lee et al., 2017). The water-energy nexus concept was later extended by taking the corresponding greenhouse gases into account. The comprehensive approach was referred as water-energy-carbon (WEC) nexus (Chhipi-Shrestha et al., 2017). An integrated local production network was studied by Leung Pah Hang et al. (2016) to overcome a plethora of social and environmental issues using the WEC nexus concept. The nexus between energy, water, and carbon has been recently generalized to include large-scale food-related sectors (Karan et al., 2018; Kılkış and Kılkış, 2017; Yang et al., 2017). Although much progress has been made to revise international or national policies based on the WEC nexus reports, a model-based application of the methodology is rare. In such an application, the systems could be optimized, monitored and analyzed regardless of the local policies and operational restrictions.

The dynamic nature of the WEC nexus requires a robust

* Corresponding author.
E-mail address: ckyoo@khu.ac.kr (C. Yoo).

https://doi.org/10.1016/j.jclepro.2018.10.150
0959-6526/© 2018 Elsevier Ltd. All rights reserved.

mathematical framework. Therefore, algebraic approaches were used to simplify the complexity in a system of equations based on input-output (I/O) models. Accordingly, predefined sectors were considered as the operational units and the linkages were investigated either as the inputs or outputs of each unit (Turconi et al., 2013). Although, the I/O model was assumed to overestimate the impacts in a life cycle assessment (LCA), it was used to efficiently revise cross-country, national and multi-reginal policies (Bortolamedi, 2015; Freire-González and Font Vivanco, 2017; Shao et al., 2017). The process chain analysis (PCA) was preferred in case of a detailed life cycle assessment. However, the PCA underestimated the impacts as a result of applying a series of cut-off criteria for simplification. Thus, hybrid models were often preferred after Wiedmann et al. (2011) compared the results of the three approaches in a case study. Their study yielded an impressive conclusion on data-based LCA. However, the LCA studies on non-flexible systems lead to deterministic results such as constant coefficients, indices and quantities. Subsequently, deterministic regulations were set to eliminate environmentally hazardous facilities that resulted in considerable economic and social disadvantages. It goes without saying that a smart application of controlled systems could reduce the socio-economic costs of the engineering systems' shut-down that has not been studied yet, in detail.

Regardless of the methodology, the LCA was traditionally treated as a supplementary analysis to evaluate the environmental performance of technically designed or operating systems. In this way, the techno-economic and environmental performances of systems were independently evaluated and the interconnections between them were neglected (Moncada et al., 2018). The mathematical models were developed based on the recorded data obtained from the operating systems and the exogenous parameters were assumed to be the uncertainties of the models. Thus, the compatibility of a system with the varying environmental conditions during the life cycle was not included in the designs systematically (Mi et al., 2015). In conventional studies of this type, the environmentally hazardous technologies were usually identified and the techno-economic feasibility of proposed solutions were compared and vice versa. Thus, the systems were compared using various parameters, each of which was obtained from either of the assessments (Liu et al., 2017; Rodríguez et al., 2018). However, the LCA results were later combined with economic, exergy and ecologic analyses using novel mathematical models (Caliskan, 2015; Kunanuntakij et al., 2017; Sui et al., 2014). The combined models facilitated the analysis of model-based systems, but the inconsistencies between the LCA parameters and engineering design variables hindered the development of a uniform model that included common variables. There are two main advantages of combining the LCA and techno-economic assessments, elaborately. Firstly, a system can be technically optimized using the same variables that were identified as the weakness of the system in an LCA. Secondly, holistic management policies can be set in which the environmental and economic improvements are simultaneously monitored.

Having reviewed the relevant literature and the present research gaps, the novelties of the present study can be described. Firstly, self-sustainability analysis is defined for the water and energy systems for the first time and the corresponding flowchart is applied in a water and energy intensive system. The novel analysis surmounts the temporal boundaries between the design and operational stages taking the required water and energy at the upstream, operational and downstream stages of a production unit into account. Secondly, the nonlinear program used as the mathematical model is designed so that the system under study is optimized autonomously. Accordingly, all technical, economic and environmental aspects are mentioned in the optimal design. Thirdly, the imaginary water, energy and carbon streams between the components are added to the real flows using an algebraic I/O model to give a better insight to WEC nexus. Thus, a model-based WEC nexus is explicated regarding the linkages between the system components in a dual-layer model for the first time. Fourthly, the deterministic results obtained by conventional I/O tables are challenged by applying a manipulating variable. Subsequently, the applicability of the controlled systems is investigated to obtain a cleaner production technology considering the whole life cycle. The novel approach is validated using the real data and the sensitivity of the model is discussed with respect to the variation of a manipulating variable. Fifthly, the performance of the system in various scenarios are compared using environmental, economic and combined environmental-economic costs of products that are proposed for the first time. Employing the novel variables, a cleaner production technology is investigated in an efficient holistic approach as the main logic of the article.

2. Materials and methods

The contents of the current research are divided into three subsequent parts as shown in Fig. 1. According to the figure, the first block contains three sub-sections: water-energy-carbon (WEC) sector determination, the system configuration and boundaries, and the scenarios definition. The problem is detailed at this level and solved in the following sections. In the second block, a mathematical approach is described that includes technical, economic, and environmental models. Three models were totally integrated in a nonlinear program to design and analyze the water and energy intensive system which is referred to as a self-sustainability flowchart. Finally, the sensitivity of the model with respect to the manipulating variable was determined and a parametric applicability analysis was performed using economic, environmental and combined variables to compare the scenarios.

2.1. Problem statement

The major questions to be answered in the present study are as follow:

1 Which fuel is sustainable considering combined environmental-economic costs in a cradle-to-grave life cycle; coal or natural gas?
2 How do renewable energies contribute to the energy generation considering both economic and environmental aspects in an LCA?
3 Which production technology is cleaner and economic considering the WEC nexus concept; a single generation or a cogeneration technology?
4 What is the role of controlled facilities in minimizing the losses and hazards of anthropogenic systems?
5 How can the engineering systems be optimally designed and operated using WEC nexus- assisted mathematical models?

2.1.1. Water-energy-carbon sector determination

The WEC nexus concept relies on pathways between three interdependent sectors from an industrial point of view: the energy generation, the water production and the carbon sectors. Here, the carbon sector includes both carbon-rich fossil fuels and hazardous emissions in carbon dioxide equivalent ($CO_2 - eq$). The WEC nexus concept is graphically displayed in Fig. 2. According to the figure, energy, water and carbon sectors are separately represented using a square, an ellipse, and a triangle, respectively. The interactions are shown using colorful arrays so that red, blue and gray arrays

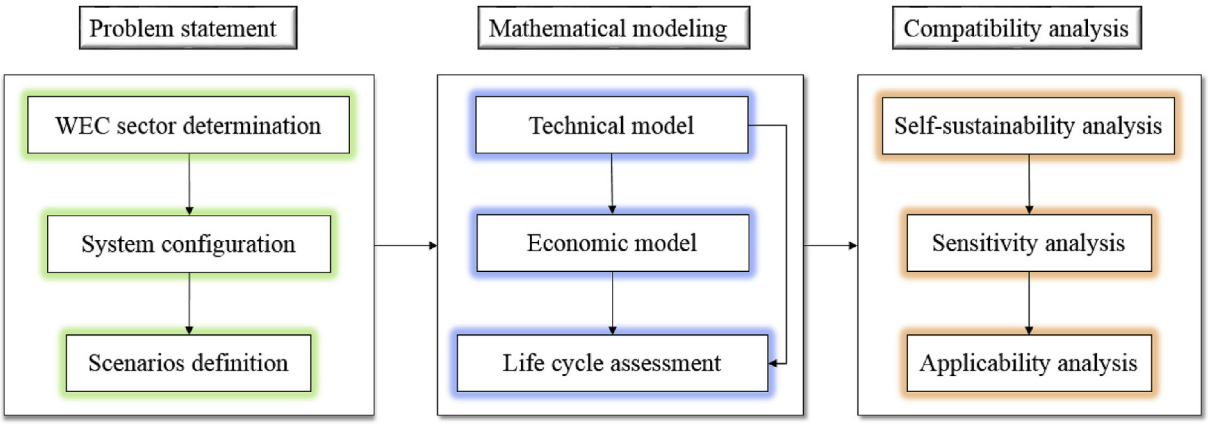

Fig. 1. Research framework.

represent energy, water and carbon outflows, respectively. Here, the mixed effect has been ignored and three main linkages are shown in the figure: internal effect (arrows beginning and ending in a sector), net backward linkages (arrows ending in a sector) and net forward linkages (arrows beginning in a sector) (Fang and Chen, 2018). The WEC nexus can be mathematically expressed using an I/O model as given in Eq. (1) (Liu et al., 2012).

$$\mathbf{T} = \mathbf{IM} \times \mathbf{T} + \mathbf{D} \tag{1}$$

where **T** is a 3 × 1 vector representing the total quantities of energy, water and carbon sectors, **IM** is a 3 × 3 interactions matrix, and **D** is the vector associated with direct energy, water production and carbon emissions. **IM** is given in Eq. (2).

$$\mathbf{IM} = \begin{bmatrix} E_E & E_W & E_F \\ W_E & W_W & W_F \\ C_E & C_W & C_F \end{bmatrix} \tag{2}$$

where E_E, E_W and E_F represent a share of the total energy required in the power plant's life cycle including the lost energy during energy conversion, the energy consumed in the life cycle of a water treatment plant (WTP) and the required energy in the fuel cycle, respectively. The arrays in the second row represent the water withdrawal amounts in the same sectors in which the distribution losses are also considered. C_E, C_W and C_F are the hazardous emissions in $CO_2 - eq$, respectively, for total energy consumption, total water withdrawal and total fossil fuel including the emissions in the fuel cycle. Each array is obtained using the mathematical model described in section 2.2.

A system's net energy and freshwater production is referred as the "direct" energy and water, respectively. The term "indirect" includes all upstream (construction), operational, and end of life (downstream) stages. Water withdrawal is defined as the amount of water removed from the ground or diverted from a water source (Macknick et al., 2011a). A fuel cycle is assumed to consist of fuel extraction, processing, transportation and distribution. Direct emissions are in the operational stage and indirect emissions refer to the fuel cycle.

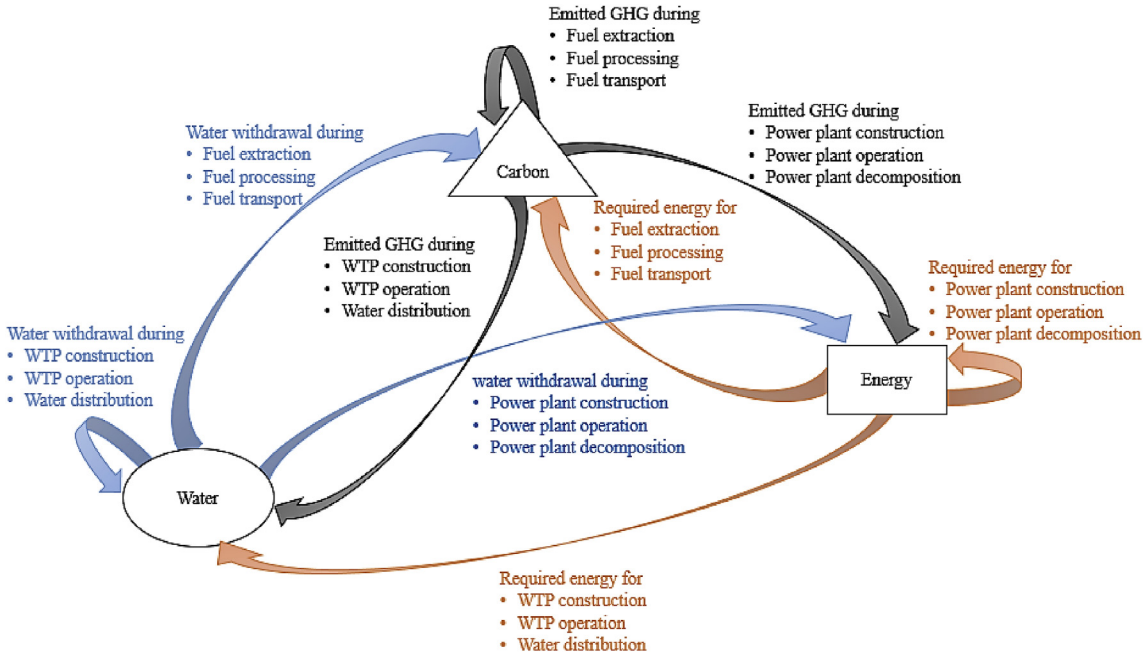

Fig. 2. Water-Energy-Carbon nexus.

2.1.2. System configuration and boundaries

Coal and natural gas are expected to remain the most common fossil fuels used in global power generation until 2035, representing 32% and 21% of the total, respectively. The share of the renewable energies strongly depends on fragile international agreements that are of concern to conservative policy makers. On the other hand, wet cooling towers have considerable water usage among non-renewable energy systems (Meldrum et al., 2013; Turconi et al., 2013). Thus, a system consisting of these energy and water intensive technologies accompanied by challenging renewable systems was studied. The system is shown in Fig. 3.

According to the figure, the system consists of a hybrid renewable energy system (HRES), a non-renewable energy system (NRES), a reverse osmosis (RO) module, and a fuel cycle. The HRES consists of solar photovoltaic (PV) modules connected to converters and a wind turbine (WT) farm indicated as a green square. The RO module consists of the pumping station and RO stages. The module provides the whole system with the required freshwater, which is shown as a blue square. The fuel production units are indicated in dark black lines. A Rankine cycle-based steam power plant, an absorption heat pump, and a wet cooling tower were integrated to form the NRES. The NRES was fueled by the hot stream provided in a furnace (Furn.). A full discussion of the thermodynamic properties of the NRES was published by Ifaei et al. (2016b). The only change to the system was that the solution valve of the heat pump was replaced with a control valve (CV) that facilitates control of the power plant's thermodynamic behavior.

The black arrows show the real hydraulic streams in Fig. 3, whereas the imaginary energy, water and carbon flows are schematically represented by red, blue and black arrows among the subsystems, respectively. The real streams are used in the first layer of the self-sustainable model for techno-economic analysis. The imaginary streams are used in the second layer after the LCA and the techno-economic analyses are integrated using the I/O model, as detailed in section 2.1.1. The boundaries between the system and the environment are shown in dotted black lines.

2.1.3. Scenario definitions

The system described in the previous section was investigated using four scenarios which are detailed as follows:

Scenario I: The required direct and indirect energies are provided only by the NRES. Hence, the HRES is eliminated in this scenario. The feedwater was assumed to be seawater so the NRES is an onshore plant. All water requirements were supplied by the RO module which was run using the power provided by the NRES. The required fuel was assumed to be pulverized coal. So, coal mining, processing and transportation were taken into account as the fuel cycle. It was assumed that a surface mining process was employed and the only coal transportation option was by rail (Mintz et al., 2015; Spath et al., 1999).

Scenario II: NRES was the only energy generation system. The water production was the same as described in scenario I. However, the fuel was assumed to be conventional natural gas and the extraction, processing and distribution of a conventional natural gas case was investigated. It was assumed that the natural gas was conveyed using pipelines in gas form and no liquid form shipping or shale gas drilling was considered (Burnham et al., 2012).

Scenario III: HRES was also used in addition to the NRES to provide the required electrical power. The total required energy was divided into two equal parts each supplied by one of the energy production systems. The input solar and wind energy to the boundaries of the system were not considered as energy inputs and only the converted energy by the HRES was

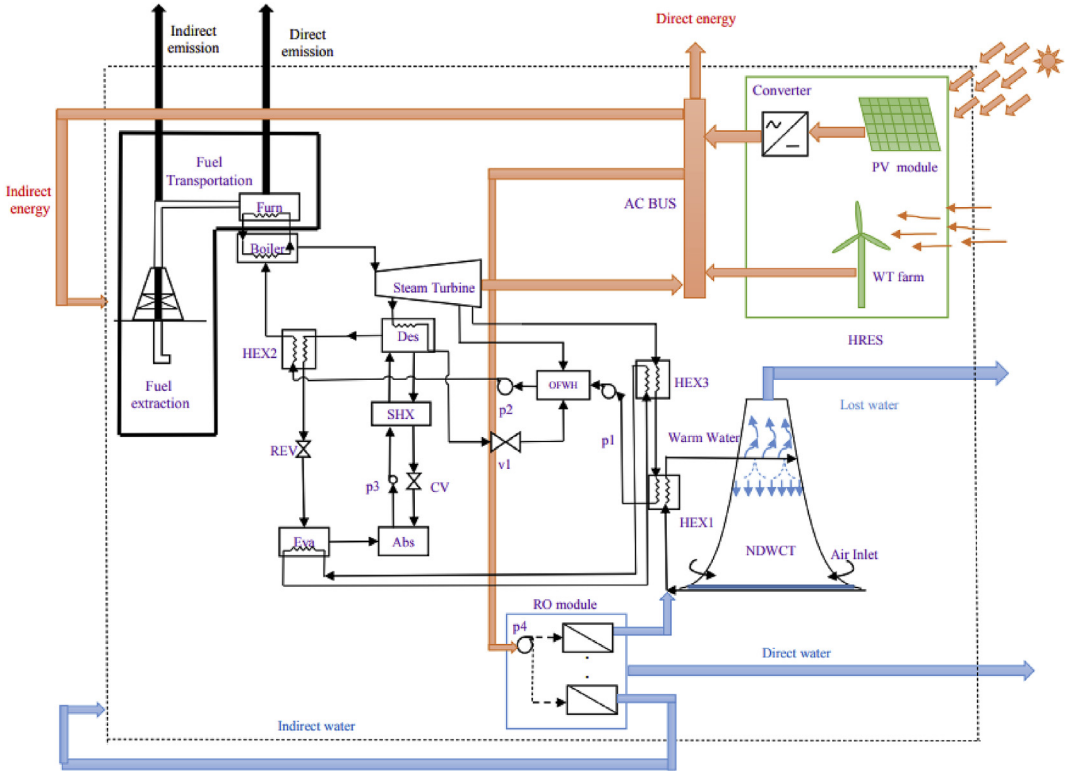

Fig. 3. System configuration and boundaries.

investigated. The NRES was fueled using natural gas and the water requirements were provided as discussed in scenario II.
Scenario IV: Unlike the previous scenarios where the net energy was the only useful product of the system, a cogeneration system was discussed in this scenario. Thus, the capacity of the desalination subsystem was increased so that the net freshwater was the second product after the water requirements of the system were met. Natural gas was the fuel and the HRES was not included as it was not in the second scenario.

The scenarios were defined according to the major questions listed in section 2.1. Since all variables were fixed except the fossil fuel, the first question could be answered comparing the results of scenarios I and II. The answers to the second and the third questions would be obtained with respect to the results of scenarios III and IV, respectively.

2.2. Mathematical modeling

2.2.1. Techno-economic model

The modeling equations developed by Ifaei et al. (2016b) and Nafey and Sharaf (2010) and the corresponding simplifying assumptions were used to construct the thermodynamic models of the subsystems.

The modeling equations are summarized in Table 1 and the corresponding variables are given in the nomenclature. The major equations of the NRES are presented in Eqs. (3)–(9). The NRES performance criteria were obtained using Eqs. (10) and (11).

$$\dot{W}_{NRES} = \sum \dot{W}_{turb} - \sum \dot{W}_{op} - \sum \dot{W}_{up} \tag{10}$$

$$\eta_{NRES} = \dot{W}_{NRES} \Big/ \dot{Q}_{in} \tag{11}$$

where $\dot{W}_{NRES}$ is the direct power of the NRES product, $\dot{W}_{turb}$ is the power obtained from each turbine, $\dot{W}_{op}$ is the required operational power and $\dot{W}_{up}$ is the indirect power consumed to supply the required energy upstream. $\dot{Q}_{in}$ is the thermal power supplied in the furnace to generate the hot external hot steam.

The RO module was modeled using Eqs. (12) through (20). The RO subsystem was evaluated in terms of the required power in the RO pump ($\dot{W}_{RO}$) and specific power consumption (SPC) as given in Eqs. (21) and (22).

$$\dot{W}_{RO} = \left(\dot{m}_f \times \Delta P \times 1000\right) \Big/ \left(3600 \times \rho \times \eta_{pump}\right) \tag{21}$$

$$SPC = \dot{W}_{RO} \Big/ \dot{m}_d \tag{22}$$

where ρ is the density and η_{pump} is the pump's isentropic efficiency (Ifaei et al., 2016b).

The HRES consisted of two weather-driven technologies: solar PVs and WTs. Accordingly, the required datasets and modeling equations were obtained from Ifaei et al. (2017a). The average quantities of the annual hourly global horizontal radiation, wind speed, and temperature at the thirty stations were scaled in daily average quantities which can be found in the supplementary file. The major modeling equations are given in Eqs. (23) through (30) in Table 1 and the variables' description can be found in the nomenclature.

The economic model of the NRES was developed based on the nonlinear equations summarized in Table 2. According to the table, the purchased equipment costs (PEC) were obtained using Eqs. (31) through (37). The PECs were obtained in various referenced years so they are updated to a more recent time using Eq. (38) (Safder et al., 2018).

Table 1
Major equations of the technical model.

Equations	NO.
NRES	
$\dot{W}_{turb} = \sum \dot{m} \times (h_{in} - h_{out})$	(3)
$\eta_{pump} = \dfrac{\dot{m}_{pump} \times v \times (P_{out} - P_{in})}{\dot{W}_{pump}}$	(4)
$\sum_{i=1}^{n} (\dot{m}_i \times h_i)_{in} = \sum_{j=1}^{m} (\dot{m}_j \times h_j)_{out}$	(5)
$\varepsilon_{HEX} = \dfrac{\Delta T_{\min}}{(T_h)_{in} - (T_c)_{in}}$	(6)
$SgV = (\dot{m}\, c_p)_{cold} - (\dot{m}\, c_p)_{hot}$	(7)
$h_{in} = h_{out}$	(8)
$(\dot{m}_{valve})_{in} = (\dot{m}_{valve})_{out}$	(9)
RO	
$\dot{m}_f = \dot{m}_d / SRR$	(12)
$X_d = X_f \times (1 - RR)$	(13)
$\dot{m}_f = \dot{m}_b + \dot{m}_d$	(14)
$\dot{m}_f \times X_f = \dot{m}_b \times X_b + \dot{m}_d \times X_d$	(15)
$P_i = 75.84 \times X_i$	(16)
$\Delta\Pi = \Delta\Pi_{av} - P_d$	(17)
$\Delta P = \left(\dfrac{\dot{m}_d}{3600 \times TCF \times FF \times N_e \times N_v \times A_{memb} \times K_w}\right) + \Delta\Pi$	(18)
$K_w = (6.84/10^8) \times (18.6865 - (0.177 \times X_b)))/(T_f + 273)$	(19)
$TCF = exp(2640 \times ((1/298) - 1/(273 + T_f)))$	(20)
HRES	
$\dot{W}_{PV} = Y_{PV} f_{PV} \left(\dfrac{G_T}{G_{T,STC}}\right) \left[1 + \alpha_P (T_C - T_{C,STC})\right]$	(23)
$T_C = \dfrac{T_a + (T_{C,NOCT} - T_{a,NOCT}) \left(\dfrac{G_T}{G_{T,NOCT}}\right) \left[1 - \dfrac{\eta_{mp,STC}(1 - \alpha_p T_{C,SCT})}{\tau.\nu}\right]}{1 + (T_{C,NOCT} - T_{a,NOCT}) \left(\dfrac{G_T}{G_{T,NOCT}}\right) \left(\dfrac{\alpha_p . \eta_{mp,SCT}}{\tau.\nu}\right)}$	(24)
$G_T = (G_g - G_d).R_b + G_g.g_a.\dfrac{(1 - \cos\beta)}{2} + G_d R_d$	(25)
$\eta_i = \dfrac{\dot{W}_{out,i}}{\dot{W}_{in,i}}$	(26)
$\dot{W}_{WT} = \dot{W}_{theory}(1 - F_{total})$	(27)
$\dot{W}_{theory} = {}^1\!/_2 \rho_{hub} . {V_{hub}}^3 . A . C_P$	(28)
$\rho_{hub} = \dfrac{\bar{P}}{R_d . \bar{T}}$	(29)
$\dfrac{V_{hub}}{V_{anem}} = \dfrac{\ln\left(Z_{hub}/Z_0\right)}{\ln\left(Z_{anem}/Z_0\right)}$	(30)

$$CC_{2016} = CC_{ref} \left(CI_{2016} \Big/ CI_{ref}\right) \tag{38}$$

where CI is the chemical engineering plant cost index and the subscript ref represents the referenced year.

A linear program was developed to obtain the cost of the RO plant. The major costs equations are given via Eqs. (39) through (53) and the corresponding variables description can be found in the nomenclature. The systems' economic criteria were obtained using Eqs. (54) through (56).

$$TAC = ACC + AOC \tag{54}$$

$$ACC = TCC \times CRF \tag{55}$$

Table 2
Major equations for the economic model.

Equations	No.
NRES	
$CC_{boiler} = 205 \times (H_b^{-0.13})$	(31)
$CC_{OFWH} = 66 \times Q \times \left(\left(\frac{1}{\Delta T_{OFWH} + a_4}\right)^{0.1}\right)$	(32)
$CC_{pump} = 308.9 \times (\dot{W}_{pump})^{Cof_{pump}}$	(33)
$CC_{turb} = 3880.5 \times (P_{turb}{}^{0.7}) \times \left(1 + \left(\left(\frac{0.05}{1-\eta_{turb}}\right)^3\right)\right) \times \left(1 + 5 \cdot exp\left(\frac{T_a - 866}{10.42}\right)\right)$	(34)
$CC_{HEX,2000} = CC_{ref,HEX} \times (A_{HEX}/A_{ref,HEX})^{0.6}$	(35)
$UA_{HEX} = (\dot{Q}_{HEX}/\Delta T_{lm})$	(36)
$CC_{NDWCT} = x_1 \dot{m}_w^{x_2} 10^{x_3 TD.R + x_4 TD + x_5 R + x_6}$	(37)
RO	
$CC_{swip} = 996 \times (\dot{m}_f)^{0.8}$	(39)
$CC_{equip} = C_{pump} + CC_{swip} + CC_{memb}$	(40)
$CC_{site} = 0.25 \times DCC$	(41)
$CC_{instal} = 0.2 \times CC_{equip}$	(42)
$DCC = CC_{equip} + CC_{site} + CC_{instal}$	(43)
$ICC = 0.27 \times DCC$	(44)
$CC_{civil} = 0.2 \times CC_{PEC}$	(45)
$CC_{conti} = 0.15 \times CC_{PEC}$	(46)
$CC_{eng} = 0.15 \times (CC_{conti} + CC_{civil} + CC_{PEC})$	(47)
$TCC_{RO} = CC_{PEC} + CC_{civil,const} + CC_{conti} + CC_{engg} + DCC + ICC$	(48)
$OM_{labor} = (N_{labor}) \times (11,000) + (lf \times 0.01 \times \dot{m}_d \times 8760)$	(49)
$OM_{power} = lf \times 0.06 \times SPC \times \dot{m}_d \times 8760$	(50)
$OM_{insur} = 0.06 \times TCC \times lf \times CRF$	(51)
$OM_{chm} = lf \times 0.04 \times \dot{m}_d \times 8760$	(52)
$OM_{memb} = ((CC_{mem} \times N_e \times N_v)/lt_{memb})$	(53)

$$CRF = \frac{ir.(1+ir)^{lc}}{(1+ir)^{lc} - 1} \tag{56}$$

where *TAC* is the total annualized cost, *ACC* is the annual capital cost, *AOC* is the annual operation cost, *CRF* is the amortization factor, *ir* is the interest rate, and *lc* is the life cycle. All the required constants for the techno-economic model are summarized in Table 3.

2.2.2. Life cycle assessment

The goal of the life cycle assessment (LCA) was to obtain the required energy and water and the corresponding hazardous emissions for the above-mentioned system. The embodied water and energy in the raw materials, process energies, and the end of life energy were investigated in a cradle-to-grave approach to obtain the required water and energy in the life cycle of the system as detailed in the international standards of the ISO 14040 series (Song et al., 2018).

An inventory of the required energy and water in each stage of the processes is given in the supplementary file. According to the inventory, the main materials and the corresponding water and energy intensities are summarized in Table 4. Three subsystems that were described in section 2.1.2 are individually discussed in the table based on a process chain analysis (PCA). The required materials for the construction and operation of the subsystems were obtained from the relevant literature (Ashby, 2012; Ciferno, 2008; Fu et al., 2015; Hou et al., 2016; Meier, 2002; Nitkiewicz and Sekret, 2014; Raluy et al., 2004; Stokes and Horvath, 2009; White and Kulcinski, 2000). Mean values were employed when a range was supplied for any quantity. The quantities of the inventory were normalized to a product unit of the system in its life cycle. Rare elements and the non-standard production processes were ignored. The major assumptions in the materials inventory are as follows:

Table 3
Constants for the techno-economic model.

Model constant	Value	Unit
CI_{2016}	541.7	–
CI_{2000}	394.1	–
U_{HEX}	2.5	–
$U_{evaporator}$	1.5	–
$U_{absorber}$	0.7	–
ir	15	%
lc	25	years
N_{labor}	8	–
$A_{ref,HEX}$	100	m^2
lf	0.9	$year^{-1}$
η_{pump}	0.9	–
lt_{memb}	5	years
A_{memb}	35.3	m^2
X_f	45,000	ppm
f_{PV}	80	%
Y_{PV}	1	Kw
α_P	- 0.5	%/°C
$T_{C,STC}$	47.5	°C
$\eta_{mp,SCT}$	11.9	%
g_a	20	%
β	0	degrees
lt_{inv}	10	years
F_{total}	17.7	%
Z_{hub}	5	m
η_i	96	%
η_{PV}	13.1	%
z_0	0.2	m
CC_{memb}	1000	US $
$CC_{desorber}$	17,500	US $
$CC_{absorber}$	16,500	US $
CC_{valve}	3000	US $
$CC_{evaporator}$	16,000	US $
$CC_{condenser}$	8000	US $
$CC_{ref.HEX}$	12,000	US $
$CC_{PV,inv}$	3500	US $/kw
OC_{PV}	25	US $/kw
CC_{WT}	4000	US $/kw
OC_{WT}	60	US $/kw

Table 4
Life cycle materials inventory and the corresponding energy and water intensities.

Material	Subsystem			Energy intensity[c]			Water intensity[c]
	NRES[a]	HRES[a]	RO[b]	Upstream	Processing	Downstream	
Aluminum	3.54	19.4	–	210	16.65	26	992.5
Acids-hydroxides	–	8	0.081	2.35	0.32	1.97	1.32
Ammonia	–	0.075	0.008	0.6	28.26	5.86	1.1
Argon	–	4	–	6.8	15	0.2	46.9
Aromatic polyamide	–	–	0.0004	122.5	48.7	22	265
Bitumen	0.35	–	–	62.8	17.5	9.7	143
Brass	0.255	–	–	44	10.5	12.3	311
Carbon allotropes	–	15	–	400	42.66	32.8	420
Ceramic	0.415	–	–	2.85	0.06	0.02	5.6
CFRP	–	7.5	–	475	32.95	32	863.5
Chromium	2.765	–	–	181.5	15.85	33	592
Concrete	830	490	0.13	1.15	0.02	0.75	3.4
Copper	3.32	3.25	–	59	10	13.5	282.5
Epoxy	0.22	–	0.0001	133.5	22	30.5	214.5
GFRP	0.578	7.5	–	112.5	32.95	12.5	207
Glass	0.028	65	–	10.5	8.7	8.2	17.25
Glulam	0.005	–	–	14.5	0.503	20	750
HDPE	0.165	–	–	81	30.2	45	76
High alloy steel	0.5	–	–	222.5	14.85	35.65	309
Iron	429.6	–	–	18	10.5	10.5	26
Lead	0.135	–	–	27	5.75	7.45	350
Low alloy steel	15.42	119.2	0.12	32.5	21.95	8.6	74
Low carbon steel	–	–	0.0875	26.5	0.02	7.3	46
Manganese	0.084	–	–	51.5	5.1	4.4	344
Molybdenum	0.032	–	–	452.75	78	83	1710
Nickel	0.01	–	–	181.5	15.85	33	592
Plastics	–	45.1	–	71.5	27	28.5	182
Polypropylene	0.085	–	–	79	27.7	50	199
Polyvinylchloride	1.92	–	–	59	20.6	36	81
Rock wool	4.1	–	–	53.5	2.6	20.5	6
Rubber	0.125	–	–	67.5	16	43.5	127.4
SAN	0.029	–	–	94.5	25.1	46.5	263.5
Sand	–	–	0.065	0.5	0.4	0.02	3.4
Silicon (M-Si)	–	6.1	–	684.8	259.7	1118.1	89.2
Silver	0.004	–	–	1475	9.65	155	2305
Stainless steel	39.03	–	0.0004	84.5	27.4	12	224
Tin	–	0.15	–	932.5	18.7	12.8	747.6
Vanadium	0.003	–	–	1865	927.8	742.2	289
Zinc	0.07	–	–	60	8.7	11	340.5
Wood (Hard)	–	15	–	9.25	0.502	21.5	625

[a] The quantities are in kg per nominal installed kW.
[b] The quantities are in annualized kg/m^3 of freshwater.
[c] Energy and water intensities are in MJ/kg and L/kg, respectively.

Table 5
Combustion coefficients and the corresponding multiplication factors.

Scenario	i	Pollutant	cpc[a]	mf
I	1	SO_2	9.3	80
	2	NO_x	3	50
	3	PM_{10}	0.78	67
	4	CO_2	960	1
II	1	SO_2	0.7	80
	2	NO_x	0.9	50
	3	PM_{10}	0.05	67
	4	CO_2	443	1

[a] The combustion pollutant coefficients are in g/kwh.

- An onshore wind farm and a silicon-based multi-crystalline PV were used in the HRES.
- A 20 km pipeline was employed for which the diameter of the pipes varied between 6 and 10 inches in the onshore RO subsystem.
- Reinforced concrete was employed in required steel and concrete where necessary.

More than 40 materials were investigated in this section. Thus, the required data for energy and water intensities were collected and harmonized using various datasets in addition to Eco-invent version 2 database (Althaus et al., 2007; Ashby, 2012; Bhakar et al., 2016; Blomberg et al., 2012; Fu et al., 2015; Gutowski et al., 2013). Unlike the technical properties of the materials, the eco-properties vary significantly depending on the production technology, imported ingredients, process location, required chemical compounds and the industrial restrictions. Thus, supplementary data on the referenced materials' chemical composition and general properties are given in Appendix A.

According to Table 4, the energy intensities in the material life cycles are divided into three stages: upstream, processing, and downstream. The embodied energy in the raw material extraction, production, transportation and construction was referred to as the upstream energy while the required energy for the formation, deformation, casting, fabrication and molding of different categories of materials was considered to be the processing energy. The energy consumed at the end of the life cycle of a material, both for recycling or combustion, was given as the downstream energy. The water withdrawal in a material's life cycle was given as the water intensity of the material stream. The boundaries of the LCA were determined so that the life cycle begins from the required

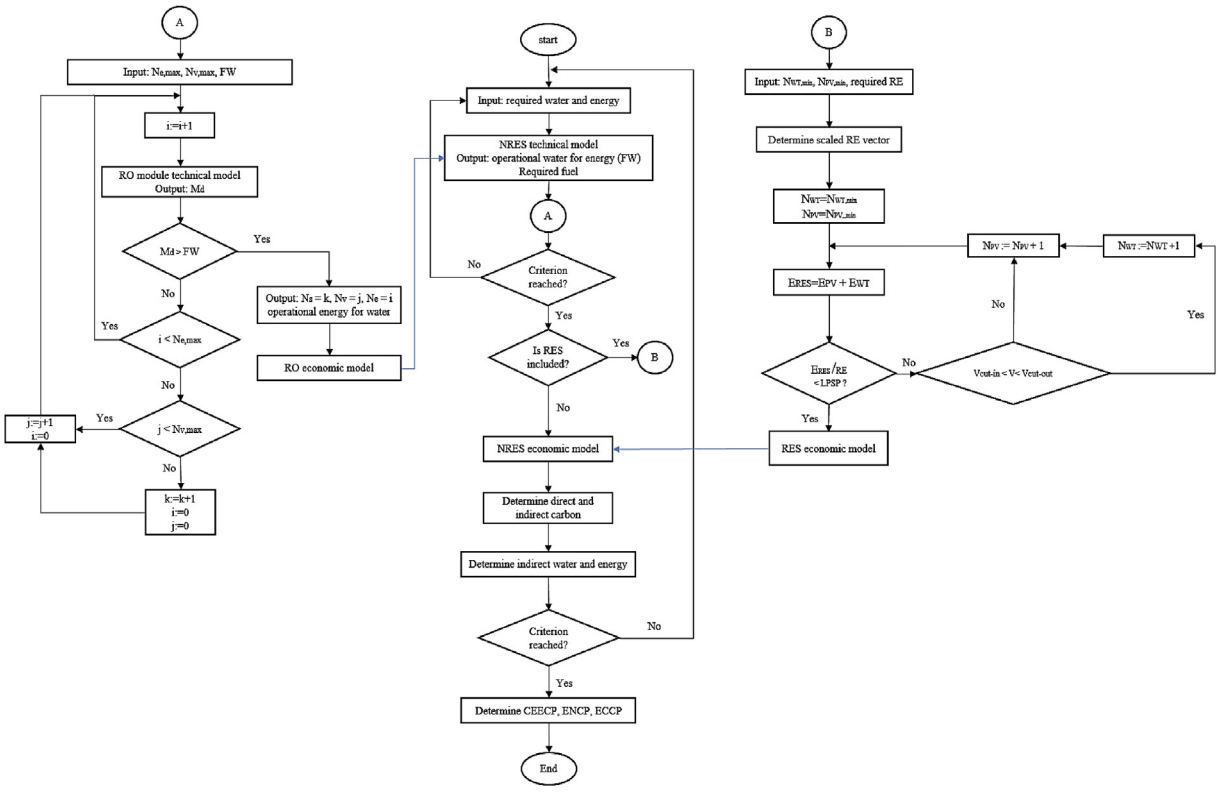

Fig. 4. Self-sustainability flowchart.

materials' industrial preparation stage. Thus, the minerals, natural creatures and the basic element life cycles were not considered in the metals, natural products and the polymer LCIAs, respectively. The energy and water in the non-operational stage of each subsystem was obtained using the inventory and Eqs. (57) and (58).

$$E_{up,sys} = \sum \left(rm \times \sum ei \right) \tag{57}$$

$$W_{up,sys} = \sum rm \times wi \tag{58}$$

where rm is the required material for each subsystem, ei and wi are the energy and water intensities of the materials, respectively.

The carbon emissions were divided into two streams in the WEC nexus calculations: direct emissions from the furnace exhaust and indirect emissions in the fuel cycle. The hazardous emissions were expressed in carbon dioxide equivalent ($CO_2 - eq$) as given in Eq. (59).

$$DC = NRE \times \sum_{i=1}^{4} (cpc_i \times mf_i) \tag{59}$$

where DC is direct carbon in $CO_2 - eq$, NRE is the annual required non-renewable energy, cpc is the combustion pollutant coefficient that is the share of each major pollutant in the mass flowrate of the furnace's chimney, mf is the multiplication factor estimated based on a 100 year life cycle of each pollutant and the subscript i denotes each of 4 major combustion pollutants. The required coefficients and factors are summarized in Table 5 (Lora and Salomon, 2005; Wu and Zhang, 2017). The NRE was obtained using Eq. (60).

$$NRE = \frac{\dot{Q}_{in} \times lc \times lf \times 8760}{\eta_{fur}} \tag{60}$$

where η_{fur} is the thermal efficiency of the furnace assumed to be 90%.

Indirect carbon refers to any hazardous emissions in the fuel cycle including mining, extraction, transportation and distribution. These stages were considered in the energy sector and only the direct releases to the atmosphere were calculated as a coefficient to the DC as given in Eqs. (61) and (62).

$$IC = \dot{m}_{fuel} \times RP \times mf \tag{61}$$

$$\dot{m}_{fuel} = \frac{NRE}{LHV_{fuel}} \tag{62}$$

where IC is the indirect carbon, RP is the released portion, $\dot{m}_{fuel}$ is the annually required fuel, and LHV_{fuel} is the lower heating value of the fuel, which is 6154.5 kWh/ton and 1031 MMbtu/m^3 in scenarios I and II, respectively (Ou et al., 2016). The RP is governed by the methane releases in the fuel cycle which was assumed to be 1.4% and 0.5% in scenarios I and II, respectively. The mf was assumed to be 25 for methane (Meier et al., 2005; U.S.EPA, 2016).

The PCA underestimates the required water and energy in the fuel cycle dramatically because the latent heat in the machinery and losses at the infrastructure of the fuel cycle are ignored (Meier et al., 2005). Thus, an economic input/output (EIO) tool was employed to estimate the water withdrawal and energy requirement in the fuel cycle. The EIO-LCA tool assesses the required water and energy based on the economic activity among 428 economic sectors using input-output models (Ou et al., 2016). The results

Table 6
Self-sustainable model validation.

Parameter	Unit	Model	Literature	Reference
Required energy in coal fuel cycle	GJ/MW	2030	2317	(White and Kulcinski, 2000)
			3400	(EIO-LCA, 2017)
Required water in coal fuel cycle	Gal/ton	167.8	22-2211	(Ou et al., 2016)
			514.4	(EIO-LCA, 2017)
Required energy in gas fuel cycle	GJ/MW	6840	7300	(Meier et al., 2005)
			11,400	(EIO-LCA, 2017)
Required water in gas fuel cycle	$Gal/MMscf$	14,422	708-5007	(Ou et al., 2016)
			44,209	(EIO-LCA, 2017)
Required water for gas-fired NRES	Gal/MWh	631.2	1200	(Meldrum et al., 2013)
			1935	(EIO-LCA, 2017)
			264-1450	(Davies et al., 2013)
			260–820	(Fthenakis and Kim, 2010)
			950-1460	(Macknick et al., 2011b)
Required water for coal-fired NRES	Gal/MWh	556.2	460-1200	(Meldrum et al., 2013)
			463–678	(Macknick et al., 2011b)
			1708	(EIO-LCA, 2017)
			290-1452	(Davies et al., 2013)
			16.3	(Ou et al., 2016)
			530-1480	(Fthenakis and Kim, 2010)
Specific power consumption in RO	kWh/m^3	5.73–6.97	2.5–7	(Siddiqi and Anadon, 2011)
			3.5–1.5	(Shalaby, 2017)
			3–5	(Nair et al., 2014)
Required energy in RO life cycle	kWh/m^3	3.23	0.39–4.82	(Stokes and Horvath, 2009)
Required energy for coal-fired NRES	GJ/MW	485	603	(White and Kulcinski, 2000
			812	(EIO-LCA, 2017)
Required energy for gas-fired NRES	J/J	2.62	2.73	(Brown and Ulgiati, 2002)
Hazardous emissions while a coal-fired NRES operation	$lbSO_x/MWh$	20.5	1.54–25.5	(Jaramillo et al., 2007)
	$lbNO_x/MWh$	6.6	2.56–9.08	(Jaramillo et al., 2007)
	gCO_2/kWh	960.03	886.8	(Hondo, 2005)
			1109.8	(Brown and Ulgiati, 2002)
	$kgSO_2/MWh$	9.3	0.3–6.7	(Turconi et al., 2013)
	$kgNO_x/MWh$	3	0.3–3.9	(Turconi et al., 2013)
	TCO_2-eq/GWh	1906	1006	(Meier et al., 2005)
			1004	(Evans et al., 2009)
			1050	(Gagnon et al., 2002)
Hazardous emissions while a gas-fired NRES operation	$lbSO_x/MWh$	1.5	0–1.5	(Jaramillo et al., 2007)
	$lbNO_x/MWh$	2	0.12–5.2	(Jaramillo et al., 2007)
	gCO_2/kWh	443	759.48	(Brown and Ulgiati, 2002)
	$kgSO_2/MWh$	0.7	0.01–0.33	(Turconi et al., 2013)
	$kgNO_x/MWh$	0.9	0.2–3.8	(Turconi et al., 2013)
	TCO_2-eq/GWh	547	443	(Gagnon et al., 2002)
			543	(Evans et al., 2009)
			466	(Meier et al., 2005)
			380–1000	(Turconi et al., 2013)
Required energy in PV life cycle	KWh/W_p	4.1	1.9	(Hou et al., 2016)
	GJ/GJ	0.24	0.17	(Meier and Kulcinski, 2002)
Required water in PV life cycle	Gal/MWh	317	1–1600	(Meldrum et al., 2013)
	Lit/MWh	1207	1470	(Fthenakis and Kim, 2010)
	Lit/kWh	1.2	0.38	(Ali and Kumar, 2017)
Required energy in WT life cycle	TJ/GWy	612	676	(White and Kulcinski, 2000)
	J/J	0.14	0.13	(Brown and Ulgiati, 2002)
	MJ/MWh	504	130–400	(Voorspools et al., 2000)
Required water in WT life cycle	Gal/MWh	269	13–83	(Meldrum et al., 2013)
	Lit/kWh	1	0.13	(Yang and Chen, 2016)
Freshwater cost	$\$/m^3$	4.97	0.7–2.8	(Shalaby, 2017)
Coal plant cost	$\$/kW$	1105	1408	(Davison, 2007)
Renewable energies cost	$\$/kWh$	0.68	0.24	(Evans et al., 2009)
Non-renewable energies cost	$\$/kWh$	0.1	0.04	(Evans et al., 2009)

obtained from EIO-LCA in the fuel cycle were calibrated using Eqs. (63) and (64).

$$W_F|_{cal.} = \left(W_{NRE}^{LCIA} \Big/ W_{NRE}^{EIO}\right) \times W_F^{EIO} \tag{63}$$

$$E_F|_{cal} = \left(E_{NRE}^{LCIA} \Big/ E_{NRE}^{EIO}\right) \times E_F^{EIO} \tag{64}$$

where $W_F|_{cal.}$ and $E_F|_{cal}$ are the calibrated water and energy in the fuel cycle, respectively. The superscripts *LCIA* and *EIO* represent the life cycle inventory analysis and economic input/output model, respectively, and the subscript *NRE* indicates the non-renewable energy system. The LHV-based fuel prices were assumed to be 2.2 $/GJ and 7.8 $/GJ in scenarios I and II, respectively (Davison, 2007).

2.3. Compatibility analysis

2.3.1. Self-sustainability analysis

In the present study, self-sustainability means that a water and energy production unit should be able to supply the required water and energy in operational, upstream and downstream stages other than the target production amount. The self-sustainability is

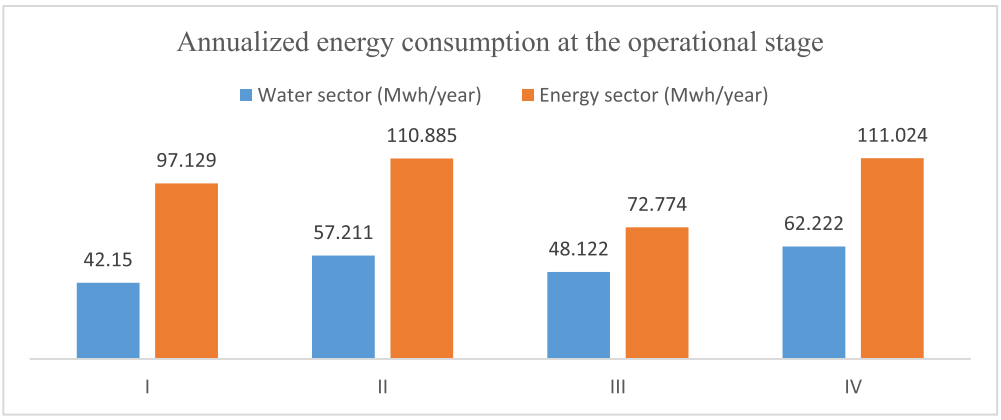

(a)

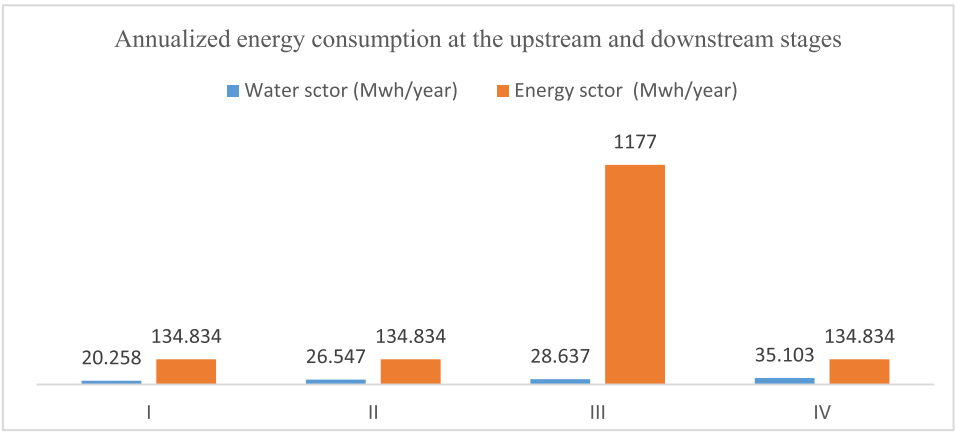

(b)

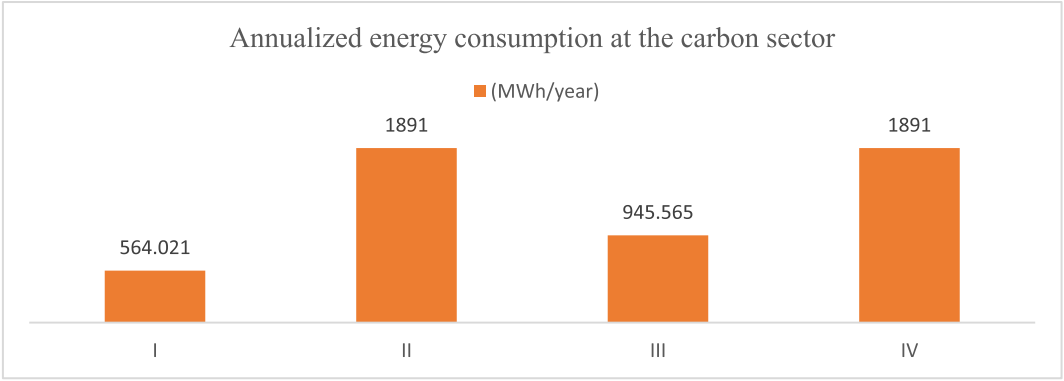

(c)

Fig. 5. Indirect energy consumption for the (a) operational stage, (b) non-operational stage, and (c) carbon sector.

measured regardless of temporal differences between the three stages. Thus, the system's product (water and energy) for the essential self-requirement consists of the losses and wastes at the operational stage as well as the upstream and downstream (non-operational) demands. According to this definition, the self-requirement is a unique value for each system, and self-sustainability analysis is not limited to local restrictions such as upstream water or energy mixes because a system is assumed to supply all its needs. Here, a nonlinear program was employed to evaluate the self-sustainability of the system which is shown in Fig. 4.

According to the flowchart, the program begins with the default input of required freshwater and energy as the products of the system. The required operational water and energy were estimated using the NRES technical model. The RO module was sized according to the required amount of water in an iterative manner. Accordingly, *i*, *j* and *k* correspond to the number of elements in a pressure vessel, vessels in a stage and the parallel stages, respectively. The $N_{e,max}$ and $N_{v,max}$ are assumed to be 6 and 50, respectively (El-Dessouky and Ettouney, 2002). Thus, the RO

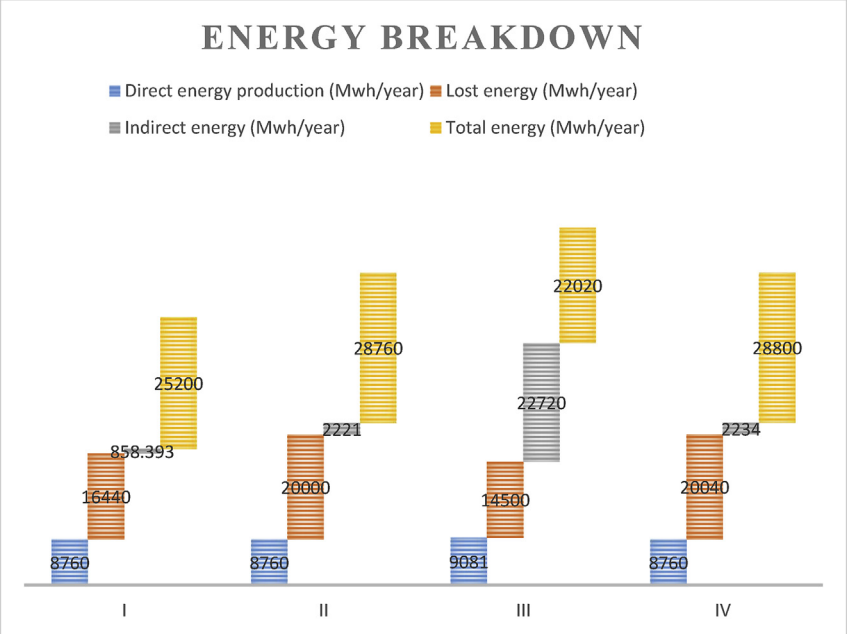

Fig. 6. An energetic comparison of the scenarios.

superstructure was optimally designed. The stop criterion to the iteration is given in Eq. (65).

$$A: \frac{X_l - X_{l-1}}{X_l} < 10^a$$
$$B: l > b \tag{65}$$

where X is the product quantity (both water and energy) and the subscript l is the iteration counter. a and b are constants assumed to be −6 and 400, respectively, according to the time required for the program to run and the precision of the model. Thus, the iteration stops if the obtained values converge in two successive iterations or the program reaches a specific number of iterations. The stop criterion hinders the reciprocal increasing of the three variables from the WEC sectors in the I/O model.

In Scenario III the HRES was also included, so the flowchart was extended to consider sub-algorithm B. The required energy is the input of the program, so it was scaled in 365 data objects as the required annual daily demand load. We assumed that the required energy was equally distributed at 500 kWh/d for simplicity. The WT was included in the configuration if the wind speed at the time step corresponds to the turbine properties. The cut-in ($V_{cut\text{-}in}$) and cut-out ($V_{cut\text{-}out}$) speed limits were assumed to be 3 m/s and 15 m/s, respectively (Mostafaeipour et al., 2013). The loss of power supply probability (LPSP) was assumed to be 0.02. The LPSP determined the optimal size of the HRES components (Ifaei et al., 2017b).

2.3.2. Sensitivity analysis

The sensitivity analysis was performed to compare the sensitivity of the model responses including total, lost and indirect values in energy, water and carbon sectors with respect to variation of the low pressure limit of the NRES (P_{low}) in each scenario. The significance of the input variable impact on the model responses was obtained by polynomial regression, and the goodness of fit was checked using multiple correlation coefficients (R^2). A first order polynomial regression was used and the slope of the polynomial equation was defined as the sensitivity of the model's output variables with respect to variation of the pressure in the CV (P_{low}) (Janghorban Esfahani et al., 2014). The output variation was recorded annually and the control range was determined using Eq. (66).

$$R = \frac{\Delta Y}{Y_{max}} \times 100 \Big|_{1.47 < P < 1.93} \tag{66}$$

where Y is the output variable and Y_{max} is the maximum quantity in the control range.

2.3.3. Applicability analysis

The parametric applicability analysis was conducted by varying the input variable in a range while keeping the rest of the variables at the baseline values (Onat et al., 2015). The input variable was the low pressure level of the NRES, which was thermodynamically controlled by means of a control valve (CV). The CV manipulated the low pressure in a range in which no changes would be required in the system's thermodynamic and hydraulic configuration (Ifaei et al., 2016a). The control range of the input variable was assumed to be between 1.47 and 1.93 kPa. The applicability of the controlled system was determined in the scenarios and the results were compared using Eqs. (67) through (69).

$$EcCP = \frac{TAC}{DE + WEF \times DW} \tag{67}$$

$$EnCP = \frac{WPC \times IW + CPC \times TC}{DE + WEF \times DW} \tag{68}$$

$$CEECP = EnCP + EcCP \tag{69}$$

where *EcCP*, *EnCP*, and *CEECP* are, respectively, economic cost of products, environmental costs of products, and the combined economic-environmental cost of the products. *WEF* is the water-energy factor determined according to the freshwater production technology and ecological circumstances. *WPC* is the environmental water penalty cost (assumed to be 0.4 \$/m^3), and *CPC* is the carbon penalty cost which is 24 \$/tones of $CO_2 - eq$(Hosseini et al.,

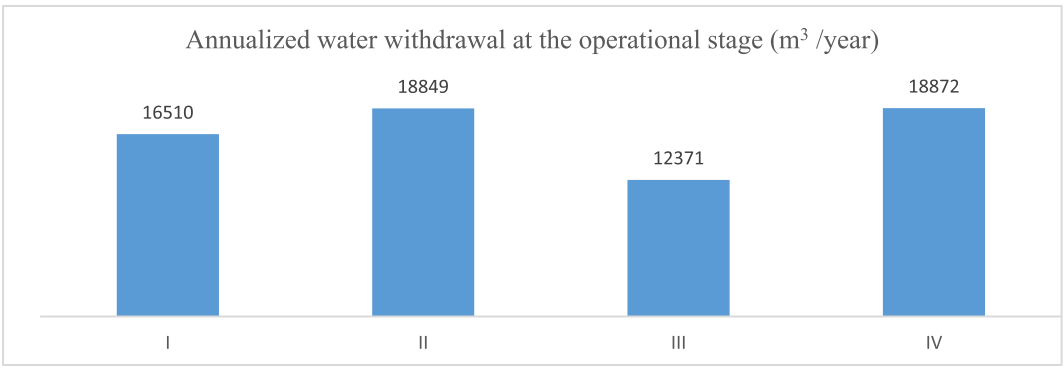

(a)

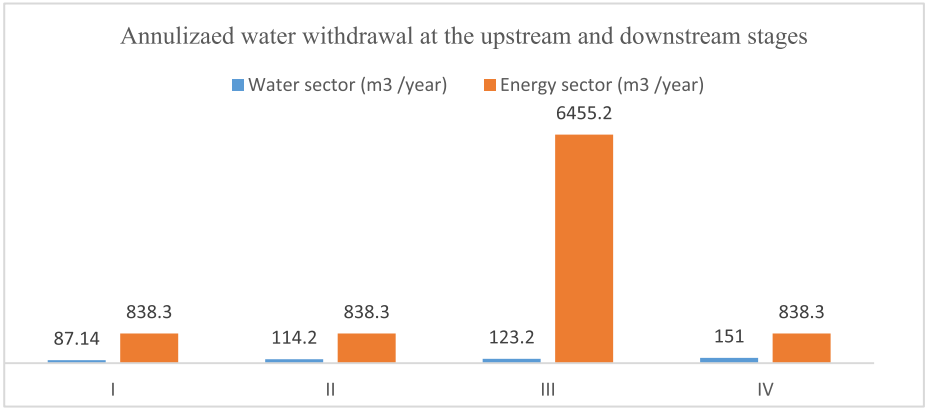

(b)

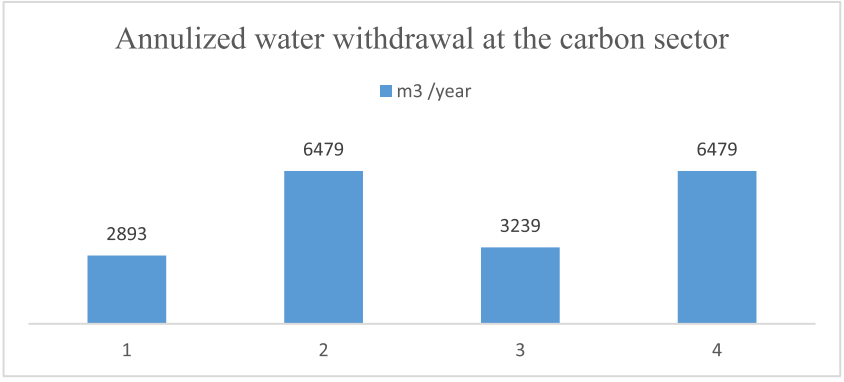

(c)

Fig. 7. Indirect water withdrawal for the (a) operational stage, (b) non-operational stage, and (c) carbon sector.

2017). Here, the *WEF* was assumed to be equal to the *SPC* of the RO module.

3. Results and discussion

3.1. Model validation and calibration

All mathematical models need to be verified and calibrated with respect to real data. Thus, the self-sustainable model was validated according to the relevant literature and the results are summarized in Table 6. The variables and units were harmonized as they appeared in the references and the conversion coefficients are given in Appendix B. The sectoral results of a single run of the self-sustainable model at the minimum low pressure level (1.47 kPa) are also given in the supplementary file.

Although the results obtained by the model were generally consistent with the previous literature, some variations were also observed. The main reason is the different assumptions and approaches employed in each article. The hazardous emissions as an instance, were often expressed as various pollutants which were combined in the self-sustainable model. The least cut-off criteria were used in the self-sustainable model so conservative outputs were obtained as a result of the holistic approach. The LCAs of the NRES and HRES were performed based on the installed capacity of the components because the HRES is highly sensitive to the weather data. Neglecting the technical and environmental

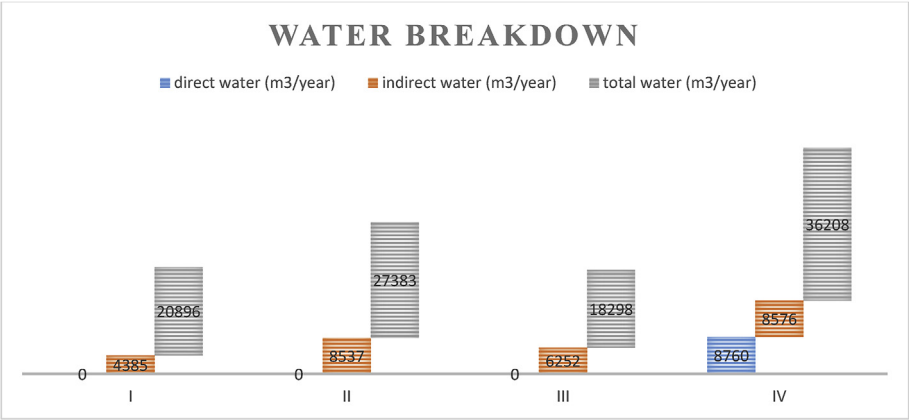

Fig. 8. A comparison of the scenarios based on annual water withdrawal.

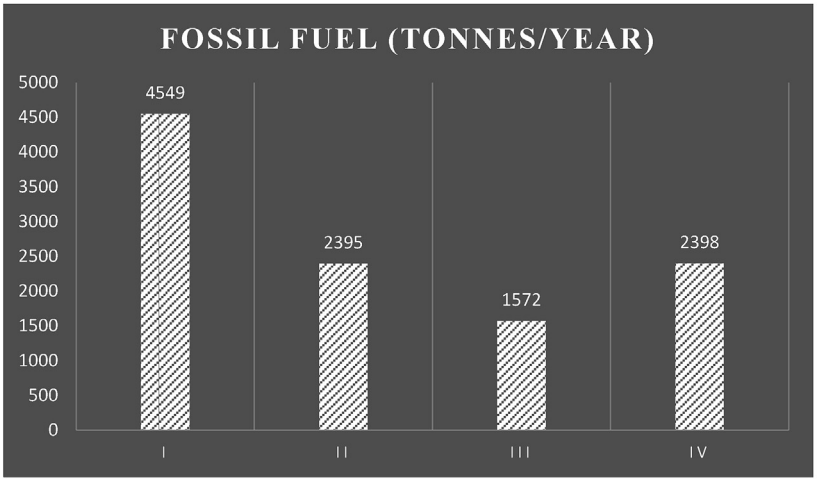

(a)

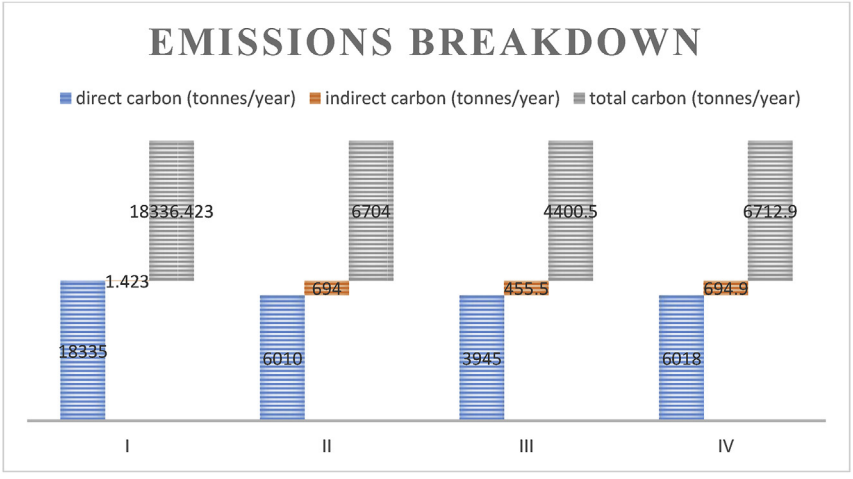

(b)

Fig. 9. A comparison of the scenarios based on annual (a) fuel consumption and (b) hazardous emissions.

restrictions in renewable energies harnessing, underestimates the required water and energy as shown in Table 6. In addition, the produced renewable energy varies significantly according to the installation location. The required solar PV and WTs in scenario III, were 2511 kW and 1352 kW, respectively, to satisfy the target demand load according to the self-sustainable algorithm. The HRES

Table 7
Water-Energy-Carbon nexus interaction matrices.

Scenario	WEC interaction matrix			
I		$E(MWh)$	$W(M^3)$	$C(Tfuel)$
	$E(MWh)$	0.66158	0.00298	0.12399
	$W(M^3)$	0.68842	0.00479	0.63596
	$C(TCO_2eq)$	0.72766	0.87754	4.03099
II		$E(MWh)$	$W(M^3)$	$C(Tfuel)$
	$E(MWh)$	0.70395	0.00306	0.78956
	$W(M^3)$	0.68454	0.00479	2.70522
	$C(TCO_2eq)$	0.23310	0.24482	2.79916
III		$E(MWh)$	$W(M^3)$	$C(Tfuel)$
	$E(MWh)$	0.65777	0.00259	0.60150
	$W(M^3)$	0.73454	0.00479	2.06043
	$C(TCO_2eq)$	0.17169	0.14897	2.79930
IV		$E(MWh)$	$W(M^3)$	$C(Tfuel)$
	$E(MWh)$	0.70437	0.00269	0.78857
	$W(M^3)$	0.68438	0.00479	2.70183
	$C(TCO_2eq)$	0.23309	0.18540	2.79942

produced 3608.83 MWh and 1646.89 MWh annually by the PVs and WTs, respectively, using the meteorological data in the supplementary file.

The required water and energy at the upstream stage of the NRES were 64,244 m^3/MW and 20,320 GJ/MW using the EIO-LCA tool, respectively. The component-based costs of the NRES used in the EIO-LCA as well as the obtained sectoral water withdrawal and energy are given in Appendix C. The same variables were calculated to be 20,958 m^3/MW and 12,135 GJ/MW following the LCIA. Thus, the calibration factors were assumed to be 0.326 and 0.597 when the EIO-LCA results were employed in the calculation of the water withdrawal and energy in the fuel cycle, respectively. As can be seen in Table 6, the self-sustainable model increases the cost of products. This is because of including the required water and energy at the upstream and downstream stages other than the requirements in the operational stages that were neglected in traditional modeling procedures.

Table 8
Results of the sensitivity and applicability analyses.

Scenario	Variable	Sensitivity	R^2	Range	Quantity	Unit
I	Total energy	457.4	99.8%	0.82%	210	MWh/yr
	Lost energy	457.3	99.8%	1.26%	210	MWh/yr
	Indirect energy	−11.2	95.1%	0.65%	5.6	MWh/yr
	Total water	−1367	95.6%	3.22%	675	M^3/yr
	Lost water	−1360	95.6%	4.04%	671	M^3/yr
	Indirect water	−6.5	95.6%	0.09%	4	M^3/yr
	Total carbon	21.1	93.7%	0.05%	10	TCO_2-eq/yr
II	Total energy	520.9	99.8%	0.82%	240	MWh/yr
	Lost energy	520.8	99.8%	1.18%	240	MWh/yr
	Indirect energy	−12.7	95.4%	0.27%	6	MWh/yr
	Total water	−1525	95.9%	2.67%	733	M^3/yr
	Lost water	−1517	95.9%	3.85%	729	M^3/yr
	Indirect water	−7.3	95.9%	0.03%	3	M^3/yr
	Total carbon	6.2	88.6%	0.04%	3	TCO_2-eq/yr
III	Total energy	344.3	99.6%	0.62%	160	MWh/yr
	Lost energy	344.3	99.6%	1.09%	160	MWh/yr
	Indirect energy	−7.6	95%	0.13%	3	MWh/yr
	Total water	−1018	95.6%	1.7%	503	M^3/yr
	Lost water	−1017	95.6%	4.04%	503	M^3/yr
	Indirect water	N	N	N	N	M^3/yr
	Total carbon	4.58	80.7%	0.04%	2	TCO_2-eq/yr
IV	Total energy	529.5	87.2%	0.86%	250	MWh/yr
	Lost energy	530.1	87.2%	1.23%	250	MWh/yr
	Indirect energy	−11.9	95%	0.27%	6	MWh/yr
	Total water	−1561	95.6%	2.12%	771	M^3/yr
	Lost water	−1553	95.6%	4.04%	767	M^3/yr
	Indirect water	−7.5	95.6%	0.05%	4	M^3/yr
	Total carbon	5.28	80.8%	0.03%	2	TCO_2-eq/yr

3.2. Water-energy-carbon nexus analysis

The WEC nexus concept was applied to the system using a sectoral I/O approach and the results were categorized according to the scenarios for an explicit comparison. The direct energy was kept the same in the scenarios, while the indirect energy changed according to the various conditions in each scenario. The annual operational energy consumption was shown in both water and energy sectors in Fig. 5 (a). The operational energy was devoted to the electrical power consumption in the pumps of the NRES and RO module. According to the figure, scenario III has the lowest operational power consumption because the HRES needs lower operational power and water compared to the NRES. The operational power has a positive correlation with the freshwater demand so the highest operational power occurs in scenario IV. The annual operational energy was 13.656 MWh greater in a 1 MW natural gas power plant in comparison with a coal-fired power plant with the same capacity. The corresponding RO module required 14.61 MWh annual energy in excess in scenario II, which had a natural gas power plant as the energy supplying unit.

As can be seen in Fig. 5 (b), the non-operational energy is approximately 8.7 times higher in scenario III, in which half the direct energy is produced by the HRES. The reasons for this are that the energy required to establish a renewable power plant is higher, the life cycle of the components in the HRES are shorter, and the efficiency of the HRES is lower than NRES. The annualized non-operational energy and water requirements were 520.26 kWh/kw and 2.97 m^3/kw, respectively, in the HRES, while the same quantities were 134.83 kWh/kw and 0.84 m^3/kw in the NRES. The energy consumption in the water sector obtained by the LCA was 35.103 MWh/year in scenario IV, which was 32% higher than that in scenario II because the module size was larger (to generate more freshwater). Although the energy sector was considered to be the same in scenarios I and II, the upstream energy was higher in the water sector of scenario II because the required total water was greater in a natural gas fired plant.

The required energy in the fuel sector is shown in Fig. 5 (c). The required energy in scenarios II and IV are almost the same proving that an increase in the RO module capacity does not contribute significantly to the required fuel. Comparing scenarios I and II, the required energy is 3.35 times greater when using natural gas. That is because the required energy for the gas extraction, distribution and processing is much higher than coal mining and transportation with the same heating value.

The energy sectors are compared in Fig. 6. According to the figure, the highest and the lowest total energies, respectively, occurred in scenarios IV (that employed cogenerated power and freshwater) and III (in which an HRES and a NRES were simultaneously applied). An energy breakdown shows that both indirect and lost energies are higher when employing natural gas in comparison with coal. The lost energy, defined by the thermal efficiency

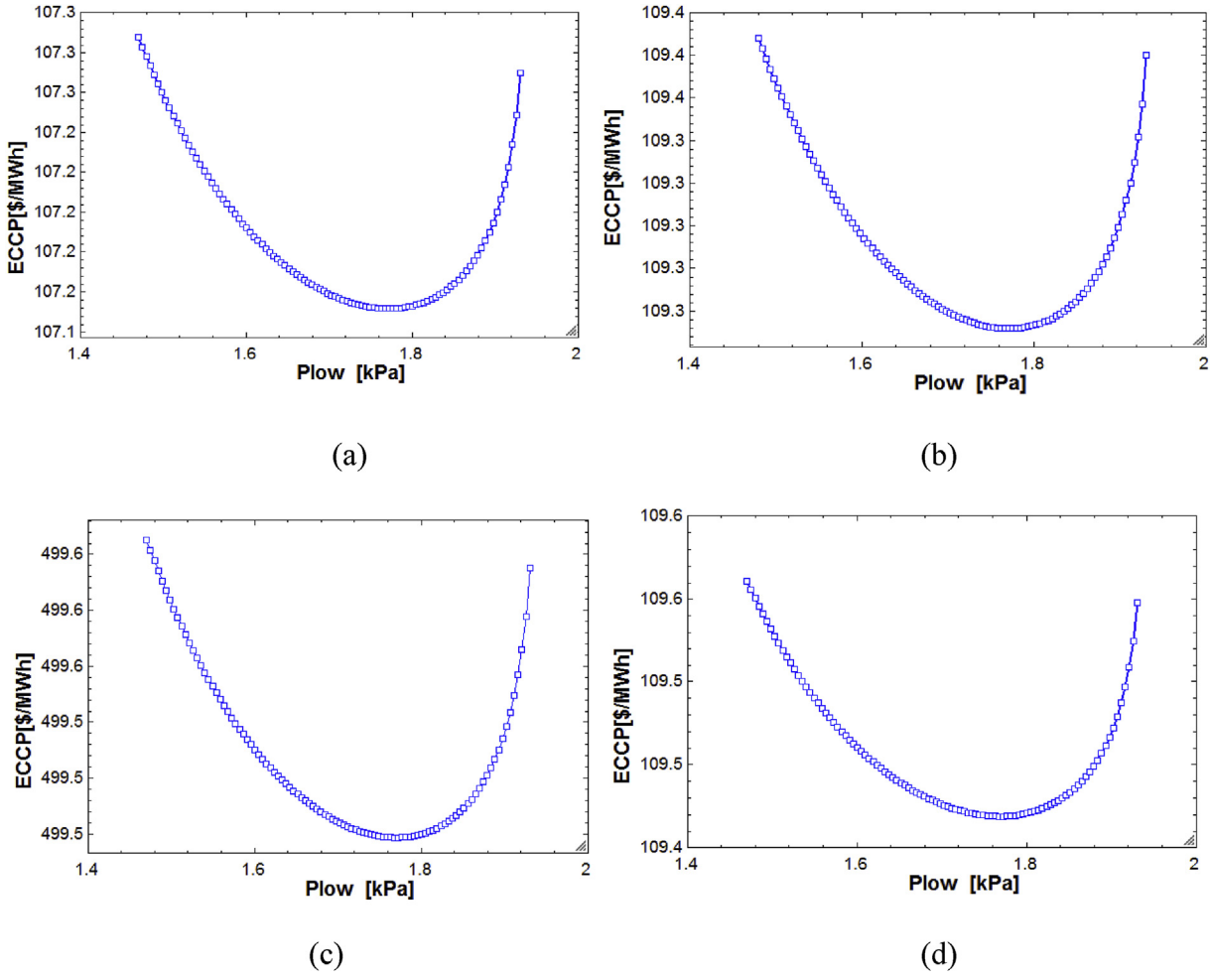

Fig. 10. Variation in the economic cost of products in the control range according to (a) scenario I, (b) scenario II, (c) scenario III, and (d) scenario IV.

of the model-based power plant, was a governing factor in the energy breakdown. As more lost energy is recovered in a system, the efficiency increases in the I/O model. The direct energy (the system product) is 321 MWh/year higher in scenario III because excess power is produced using the self-sustainable flowchart. However, the excess power was reduced using a daily average energy vector.

The indirect water withdrawals are compared in Fig. 7. According to the figure, the water withdrawals are consistent with the energy consumptions both in the operational and non-operational stages, which explains the nexus between the energy and water sectors. It can be concluded that the conversion coefficients between the water and energy systems that are frequently used in the literature are reliable based on the results of the present study. According to Fig. 7 (c), the lowest water withdrawal is observed in scenario I. Despite the fact that the required fuel is cut in a half in scenario III, the high water withdrawals in the upstream stage of the natural gas life cycle results in higher water withdrawal. The water breakdown is displayed in Fig. 8, in which the total water includes water losses in the operational stage, water withdrawals in the upstream and downstream stages of all sectors (indirect water) and the direct water as a system product. The distribution losses were considered as a multiplication factor in the upstream stage where the highest water distribution occurred. According to the figure, coal-fired plants and hybrid renewable and non-renewable systems are recommended for arid regions.

The results of the I/O model in the carbon sector are shown in Fig. 9. The carbon sector accounts for both the carbon in the fuel life cycle and the post-combustion emissions. The required fossil fuel is shown in Fig. 9 (a). The quantities are in annual tons of coal or natural gas based on the scenarios. Comparing scenarios I and II, the required coal has 1.9 times greater mass in comparison with the required natural gas. However, this fact does not result in higher energy and water requirements in the fuel cycle according to the I/O approach results. The main reason for this is that the policies in coal industries are more mature than those in the gas market. The required fuel in scenario IV is slightly higher than that in scenario II. However, this slight variation was not considerably reflected in the energy and water models.

The combustion emissions were converted to CO_2-*eq* and are shown as annual quantities in Fig. 9. According to Fig. 9 (b), the total hazardous emissions are mainly dominated by the direct emissions, which are significantly greater in scenario I. Thus, any application of coal-fired plants without considering carbon capture facilities is not recommended. On the other hand, the indirect emissions are 487 times greater in scenario II where the natural gas is extracted and distributed using conventional technologies. This quantity can be even higher for shale gas. Thus, decreasing the methane leakage in the upstream stage would lead to much better environmental protection. Scenario III has the lowest direct and indirect emissions. Thus, a hybrid application of the RES is recommended in the case of gas-fired plant operation.

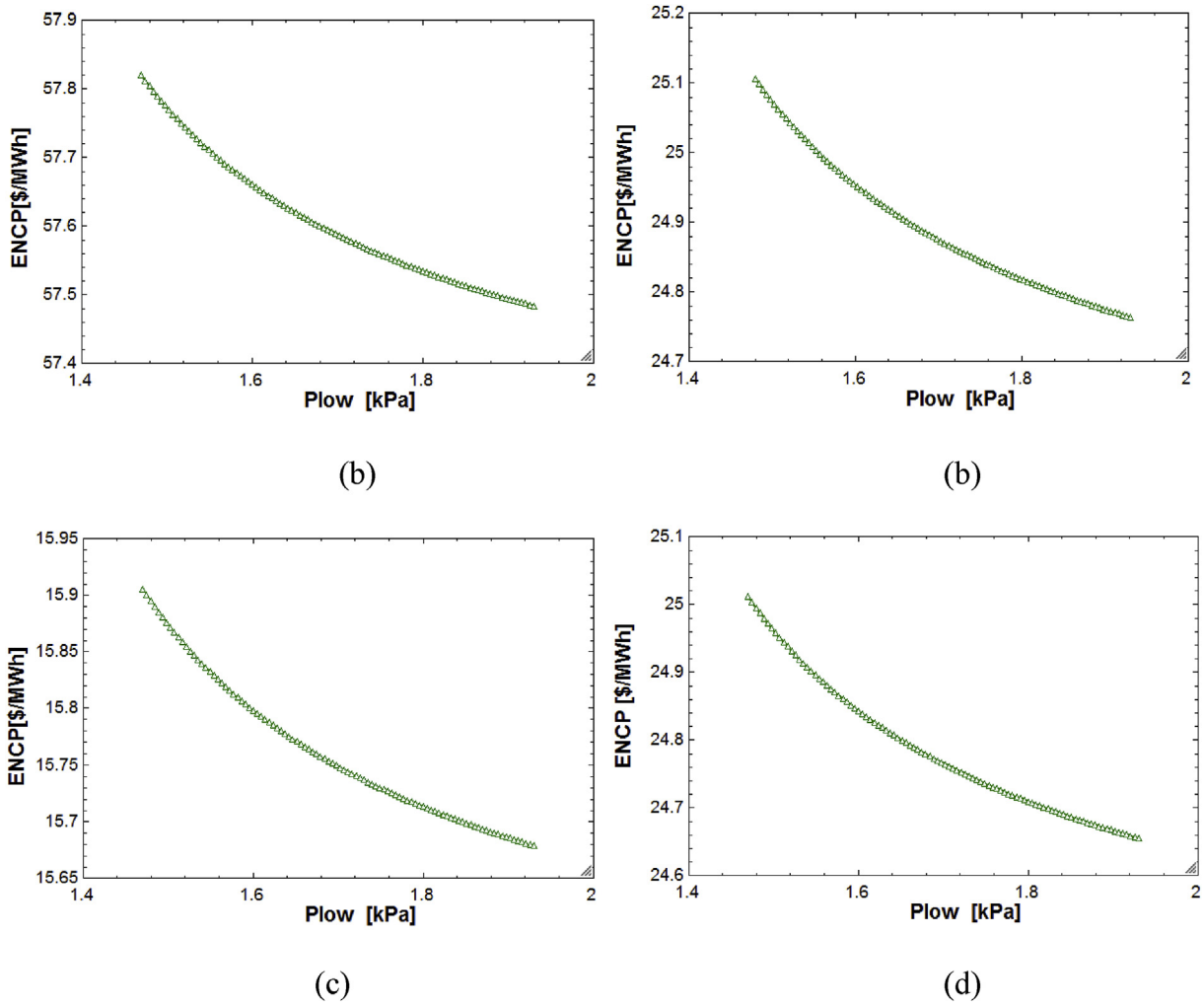

Fig. 11. Variation in environmental cost of products in the control range according to (a) scenario I, (b) scenario II, (c) scenario III, and (d) scenario IV.

Since the developed model was non-deterministic, the traditional I/O tables were replaced by algebraic equations and the WEC nexus based interaction matrices (WEC-IM) were constructed as discussed in Section 2.1.1, and the results are summarized in Table 7. The arrays of WEC-IM are consisted of the modeling equations in section 2.2 in a system of systems format. Thus, the WEC-IMs can be used to evaluate the scenarios, optimize the systems and discuss the applicability by detecting deficiencies. The rows and columns represent the inputs and outputs, respectively. The interactions implicitly express the deficiencies in a scenario such that the smaller WEC-IM arrays, indicate a more efficient system. Accordingly, the lowest E_E, E_W, C_W and C_E were obtained in scenario III as a result of the lower operational energy consumption, lower water withdrawal, lower fossil fuel requirements and smaller combustion emissions that were achieved by employing the HRES. However, the W_E was the highest in scenario III as a result of increased natural gas employment, water withdrawal upstream of the HRES and the lower efficiency of the HRES compared to the NRES. Thus, an HRES reduced the energy consumption and the corresponding CO_2-*eq* emissions in a system's life cycle, but it did not decrease the water withdrawal. The C_W and E_W were smaller in scenario IV compared to those in scenario II because of the greater freshwater production. Thus, a cogeneration system is preferred to a single generation system because of lower energy requirements and fewer hazards to the environment. Scenario I has the lowest E_C and W_C because coal was utilized as a water and energy efficient fuel. However, the quantity of C_C is significantly higher in scenario I. Thus, we concluded that retaining traditional coal mining would be logical from an economic viewpoint, but it threats sustainability in a long-term investigation.

3.3. Sensitivity and applicability analyses

The applicability of the thermodynamically controlled NRES was evaluated by manipulating the low pressure level (P_{low}) using a control valve. Although the control range was very low, 1.47–1.93 kPa, considerable variations were observed in the annual performance of the systems. This is because of the high sensitivity of the model-based systems to the variation in the low pressure limit.

The sensitivity of the model responses with respect to the manipulating variable were obtained and the results are summarized in Table 8. The corresponding graphs of each scenario are given in Appendix D. According to the table, the first order polynomial regression shows an acceptable fit for the model-based controlled variables. The best fitness occurs in scenarios I, II and IV in which the NRES is the only energy source of the system. According to the control ranges, the lost water in the cooling tower shows the highest variation range compared to other operational variables. Scenario IV has the highest variation of total carbon and

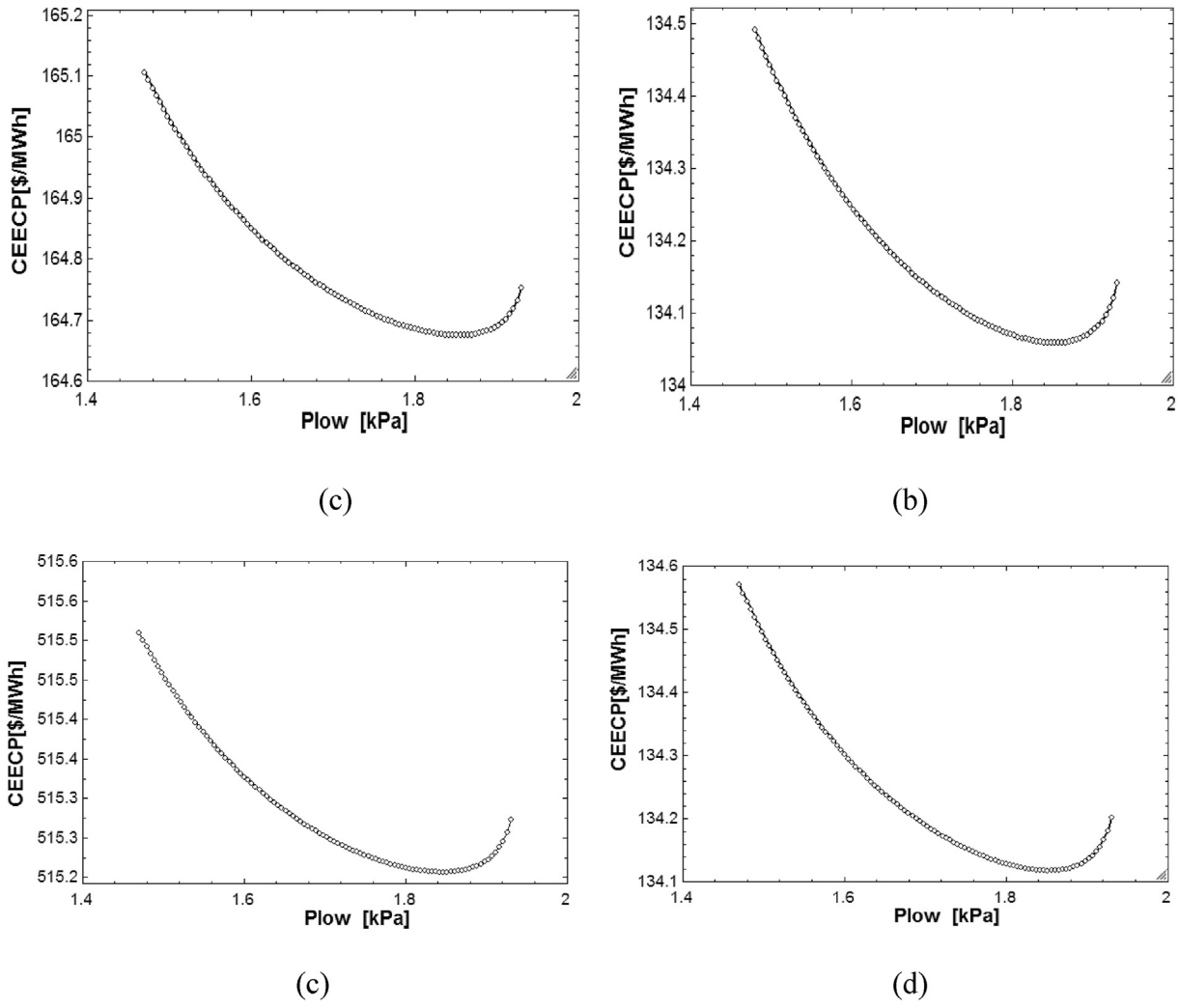

Fig. 12. The variation of combined economic-environmental cost of products in the control range according to (a) scenario I, (b) scenario II, (c) scenario III, and (d) scenario IV.

energy that means a considerable role of a flexible plant application in a cogeneration system. The highest sensitivity is observed in the water sector which has a negative correlation with the manipulating variable. In other words, as the low pressure increases, the total energy and the corresponding hazardous emissions increase but the water losses decrease. Total water savings per total carbon emitted in the control range were 67.5, 244.3, 251.5, and 385.5 m^3/TCO_2-eq, respectively, for scenarios I, II, III, IV. Thus, retrofitting the self-sustainable gas-fired cogeneration systems with the control facilities has the highest impact on water savings in dry regions. However, the optimal P_{low} could be found considering all interfering economic and environmental variables together.

The economic applicability of the system was evaluated using Eq. (67) and the results are demonstrated in Fig. 10. According to the figure, the lowest and the highest *EcCP* were obtained in scenarios I and III, respectively. This is of interest to decision makers in that it is an evaluation of the application of coal-fired power plants from an economic viewpoint. The optimal *EcCP* was obtained in a range between 1.73 and 1.76 kPa. The system's product cost can be controlled according to the market by employing the proposed NRES. The*EcCP* is slightly higher in scenario IV compared with scenario II. This means that the unit price considered for the produced freshwater and the *WEF* should be increased for logical cogeneration. Thus, the application of the cogeneration scenario is economically recommended in a dry ecology considering the proposed configuration.

The variation of the *EnCP* in the control range is displayed in Fig. 11. As can be seen, the *EcCP* decreases as the P_{low} increases in all four scenarios. That is, a higher P_{low} reduces the water losses and hazardous emissions while the production capacity is constant. The variations of *EnCP* in the control range were 0.59%, 1.41%, 1.44% and 1.46% in scenarios I, II, III and IV, respectively. Scenario I showed the lowest variation because the carbon emission costs governed the numerator of Eq. (68) in the scenario. In contrast, scenario IV had the greatest response to the controlled variable. This means that the control valve has a stronger correlation with lost water compared to the carbon emissions. Thus, the applicability of the controlled NRES is more remarkable in dry regions than in polluted areas.

The environmental and economic costs were combined using Eq. (69) and the applicability of the controlled NRES is shown in Fig. (12). As can be seen, the *CEECP* decreased by 0.4, 0.4, 0.3 and 0.5 $/MWh at the optimum pressure level. The *CEECP* of scenarios II and IV were approximately the same. This indicates that the cogeneration system can be used considering both economic and environmental costs. It goes without saying that increasing the energy and water capacities of the system reduces the costs even more. Scenario I had greater*CEECP*. That is, coal-fired plants are not recommended at all considering the environmental hazards.

Scenario III had the greatest*CEECP*, so renewable energies cannot compete with the non-renewable systems unless governmental subsides and international supports are obtained.

The main attention is devoted to the market value of products in contemporary calculation of GDP. However, an improvement can be made upgrading the GDP calculation approaches taking the environmental costs into account. In this way, the *CEECP* can be efficiently used in the future. If an expenditure approach is applied, extra taxes should be put on pollution making technologies. In this way, a green gross domestic product (GGDP) can be obtained using the *CEECP* in major economic sectors. On the other hand, incentives can be given to optimal technologies if a production approach is used to obtain the GDP. The *CEECP* is an efficient variable in both approaches because the economic growth and environment protection are considered simultaneously.

4. Conclusion

A water and energy intense system was modeled and evaluated based on the WEC nexus concept. Accordingly, the techno-economic models were combined with hybrid LCA results using a novel self-sustainable flowchart. The applicability of the controlled plant and the sensitivity of the models with respect to the variations in the manipulating variable were investigated using polynomial regression. The following conclusions were drawn according to the key questions of the article:

1 According to the fuel LCA, coal required much less energy and water than natural gas at the upstream stage that resulted in lower economic costs. However, the total emissions and*CEECP* were, respectively, 2.7 times and 22% higher in a coal-fired plant in comparison with a gas-fired power plant. Thus, natural gas was recommended for NRES considering both economic and environmental aspects in a cradle-to-grave approach.
2 Non-operational water and energies were, respectively, 7.7 and 8.7 times higher in the HRES-assisted scenario compared to other scenarios. In addition, scenario III had the lowest *EnCP* and the highest *EcCP*, simultaneously. Thus, renewable energies can replace the NRES if the market is supported by the governmental subsides.
3 Although the highest operational and total water (and energy) consumptions were obtained in scenario IV, a cogeneration system was preferred to a single generation unit. This is because of lower emissions and energy requirements in the I/O model and logical economic and environmental costs of products in cogeneration compared to that in single generation.
4 The energy and carbon sectors had a positive correlation and the water sector had a negative correlation with the manipulating variable. Hence, the optimal *CEECP* was obtained when the low pressure ranged between 1.84 and 1.88 kPa. By applying control facilities on a cogeneration plant that produces 1 MW power and 1 m^3/h freshwater, 250 MWh lost energy and 767 m^3 lost water can be annually saved. 10 TCO_2-eq/yr can also be saved using the same technique in a 1 MW coal-fired plant.
5 The LCA and techno-economic assessment were successfully integrated according to the results of the self-sustainable model validation with respect to the real data. The integrated model could then be evaluated in a higher layer of mathematical model considering the WEC nexus interconnections in an I/O model. The technical optimal conditions were obtained in a non-deterministic model taking the environmental and economic aspects into account regardless of temporal and local restrictions.

Considering the WEC nexus results, a sustainable production is achieved by the renewable energies. However, the present market can gradually adopt the changes. Thus, the current facilities can be retrofitted by the control utilities and cogeneration plants are recommended until the green technologies can compete the traditional methods.

Acknowledgements

This work was supported by a National Research Foundation (NRF) grant funded by the Korea government (MSIT) (No. 2017R1E1A1A03070713) and Korea Ministry of Environment (MOE) as Graduate School specialized in Climate Change.

Appendix A. General Properties of the materials

The general properties of the compound materials used in the LCA were summarized using the data in the Eco-invent database (version 2) and the data provided by Ashby (2012), Blomberg et al. (2012), and Gribov and Zinov'ev (2003). The data are summarized in the following table.

Table A1
General properties of the required materials

Material	Chemical composition	Density (kg/m^3)	Price (US$/kg)
Aluminum alloys	Al + alloying elements, e.g., Mg, Mn, Cr, Cu, Zn, Zr, Li	2500–2900	2.4–2.7
Acrylonitrile butadiene styrene	$(CH2–CH–C6H4)_n$	1010–1210	2.4–2.6
Bitumen	saturated hydrocarbons& (naphthenic aromatics<13 ppm, polar aromatics<9.5 ppm, asphaltenes<5 ppm)	960-1020	0.3–0.4
Butyl rubber	$(CH_2–C(CH_3)–CH-(CH_2)_2–C(CH_3)_2)_n$	900–920	3.8–4.1
Carbon fiber reinforced polymer	Epoxy + continuous HS carbon fiber reinforcement (0, +- 45, 90), quasi-isotropic lay-up	1500–1600	40–44
Cast iron	Fe/3.2–4.1%& C/1.8–2.8%& Si/< 0.8%& Mn/<0.1%& P/<0.03% S	7050–7250	0.5–0.65
Concrete	6:1:2:4 Water: cement: aggregate: Coarse aggregate	2300–2600	0.042–0.062
Copper alloys	Cu with up to 40% Zn or 30% Sn, Al, or Ni	8930–9140	7–7.6
Epoxies	$(O–C_6H_4–CH_3–C–CH3–C_6H_4)_n$	1110–1400	8–10
Hardwood: oak, along grain	Cellulose/Hemicellulose/Lignin/12% H_2O	850-1030	3–11
HDPE	$(–CH_2–CH_2–)_n$	939–960	1.7–1.9
HS carbon	Carbon, C	1800–1840	124–166
Hydrochloric acid	HCl	1003–1023	15–18
Lead alloys	Pb & 0–25% Sb or 0–60% Sn, sometimes with some Ca	11,300–11,400	2.35–2.5
Low carbon steel	Fe/0.02&0.3C	7800–7900	0.68–0.74
Low alloy steel	Fe/<1.0&C/<2.5 Cr/<2.5&Ni/<2.5& Mo/<2.5 V	7800–7900	0.9–1.1
Nickel-chromium alloys	Ni+ 10–30% Cr+ 0–10% Fe	8300–8500	33–36

Table A1 (*continued*)

Material	Chemical composition	Density (kg/m^3)	Price (US$/kg)
Nitric acid	HNO_3	1510	40–50
Plywood (Glulam)	Cellulose&Hemicellulose&Lignin&12% H2O&Adhesive	700–800	0.5–1.1
Polypropylene	$(CH2–CH(CH_3))_n$	890–910	1.85–2.05
Polyvinylchloride	$(CH_2CHCl)_n$	1300–1580	1.36–1.5
Polyester	$(OOC–C_6H_4–COO–C_6H_{10})_n$	1040–1400	4–4.4
Polyamides	$(NH(CH_2)_5CO)_n$	1120–1140	3.9–4.3
Polyester-glass composites	Epoxy + continuous E-glass fiber reinforcement (0, +- 45, 90), quasi-isotropic lay-up	1750–1970	19–21
Silver	>99.9 Ag	10,500–10,600	1850–2000
Soda-lime glass	73%SiO_2&1% Al_2O_3&17% Na_2O&4% MgO/5% CaO	2440–2490	0.8–1.7
Sodium hydroxide	NaOH	2130	0.3–0.8
Solar-grade Silicon	Si & (B < 0.1, P < 1, Al<1.4, Ti < 3.5, Fe < 11.7, C < 1000 ppm)	2329–2576	14–16
Stainless steel	Fe/< 0.25&C/16–30&Cr/3.5–37& Ni/<10&Mn + Si,P,S (+N for 200 series)	7600–8100	8.2–9.1
Stone (sand)	calcium carbonate& silicates& aluminates	2240–2650	0.3–1
Wool	Keratin (protein)	1250–1340	2.1–4.2
Zinc die-casting alloys	Zn+3–30% Al, typically, often with up to 3% Cu	4950–7000	2.4–2.6

Appendix B. conversion coefficients

The following conversion coefficients were used to convert the quantities in the British unit system to the metric unit system (Ou et al., 2016).

Table B1
Conversion coefficients

British system	Metric system
1 Gal	3.79×10^{-3} m^3
1 Gal/ton	4.17×10^{-6} m^3/kg
1 Gal/MMscf	1.34×10^{-7} m^3/m^3
1 MMscf	$2.83 \times 10^{+4}$ m^3
1 lb	4.54×10^{-1} kg
1 Gal/lb	8.34×10^{-3} m^3/kg
1 °F	$2.56 \times 10^{+2}$ K
1 MMbtu	$2.93 \times 10^{+2}$ kWh
Δ1°F	Δ0.56 K
1 Btu/lb	2.33×10^{0} kJ/kg
1 psi	$6.89 \times 10^{+3}$ Pa
1 lb/MWh	4.54×10^{-1} kg/MWh
1 ton/h	9.07×10^{-1} t/h
1 MMscf/h	$2.83 \times 10^{+4}$ m^3/h
1 Gal/MWh	3.79×10^{-3} m^3/MWh

Appendix C. Costs evaluation and EIO-LCA results

The purchased equipment costs (PEC) of the NRES components and the corresponding EIO-LCA results are summarized in the following table.

Table C1
PEC of the components and the corresponding EIO-LCA results

Component	PEC ($)	Water withdrawal (kGal)	Energy (TJ)
Turbines	2,676,000	12,600	15.4
Pumps	2129	20.8	0.021
Cooling tower	222,747	1840	2.13
Valves	1296	10.1	0.011
HEXs	213,257	2480	2.76
Total	3,115,000	16,951	20,320

Appendix D. Sensitivity analysis

The sensitivity of the model's responses with respect to variations in the manipulating variable are graphically given in Figs. D1 through D3.

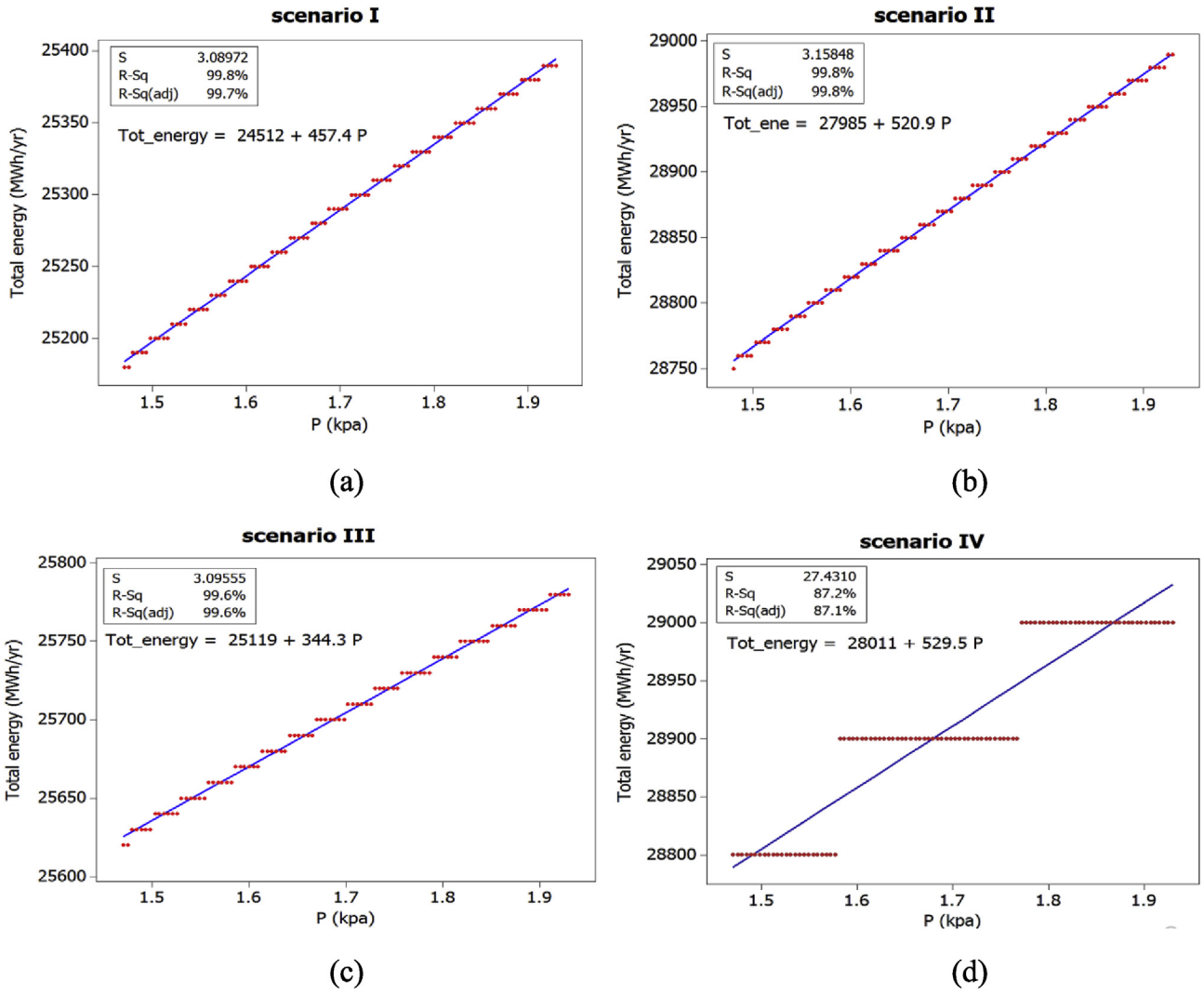

Fig. D1. Sensitivity of the total energy with respect to the low pressure limit in (a) scenario I, (b) scenario II, (c) scenario III, and (d) scenario IV.

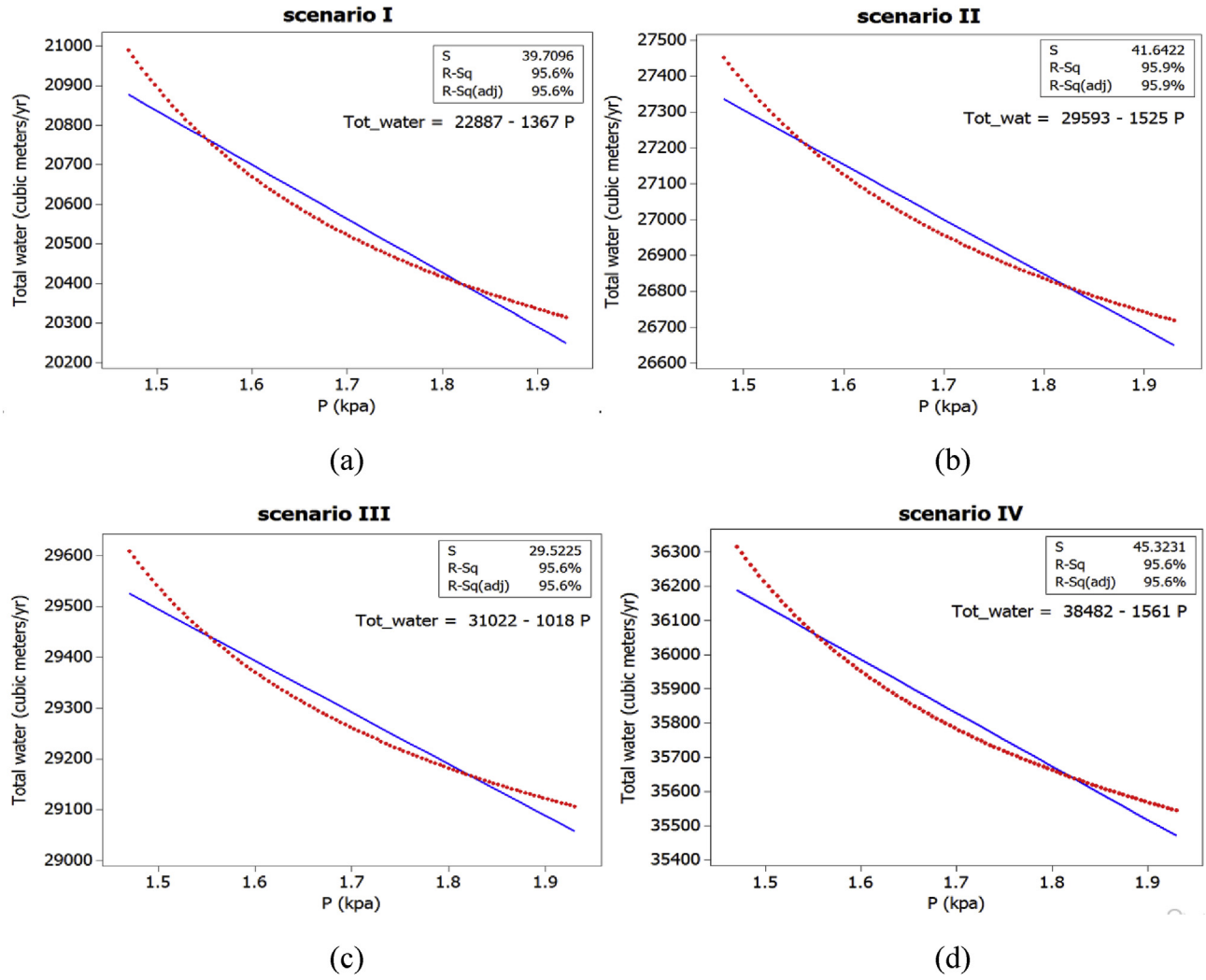

Fig. D2. Sensitivity of the total water with respect to the low pressure limit in (a) scenario I, (b) scenario II, (c) scenario III, and (d) scenario IV.

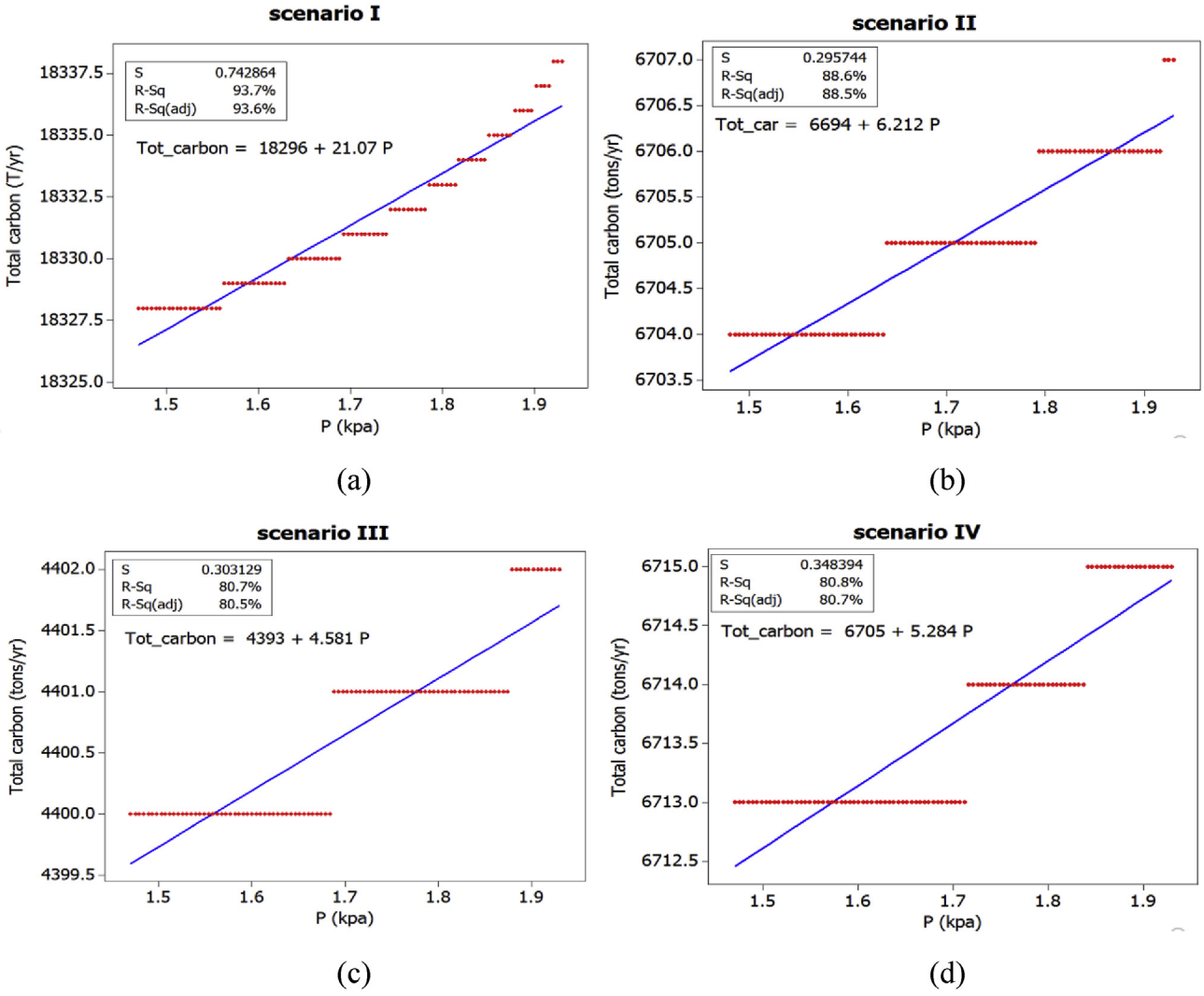

Fig. D3. Sensitivity of the total carbon with respect to the low pressure limit in (a) scenario I, (b) scenario II, (c) scenario III, and (d) scenario IV.

Appendix E. Supplementary data

Supplementary data to this article can be found online at https://doi.org/10.1016/j.jclepro.2018.10.150.

References

Ali, B., Kumar, A., 2017. Development of water demand coefficients for power generation from renewable energy technologies. Energy Convers. Manag. 143, 470–481.

Althaus, H.-J., Hischier, R., Osses, M., Primas, A., Hellweg, S., Jungbluth, N., Chudacoff, M., 2007. Life Cycle Inventories of Chemicals V2.

Ashby, M., 2012. Materials and the Environment: Eco-informed Material Choice, 2 ed.

Bhakar, V., Kumar, D.N.S.H., Sai, N.K., Sangwan, K.S., Raghuvanshi, S., 2016. Life cycle assessment of filtration systems of reverse osmosis units: a case study of a university campus. Procedia CIRP 40, 268–273.

Blomberg, T., Barnes, J., Bernard, F., Dewez, P., Clerc, S.L., Pfitzmann, M., Porot, L., Southern, M., Taylor, R., 2012. Life Cycle Inventory: Bitumen, 2 ed. eurobitume.

Bortolamedi, M., 2015. Accounting for hidden energy dependency: the impact of energy embodied in traded goods on cross-country energy security assessments. Energy 93, 1361–1372.

Brown, M.T., Ulgiati, S., 2002. Emergy evaluations and environmental loading of electricity production systems. J. Clean. Prod. 10 (4), 321–334.

Burnham, A., Han, J., Clark, C.E., Wang, M., Dunn, J.B., Palou-Rivera, I., 2012. Life-cycle greenhouse gas emissions of shale gas, natural gas, coal, and petroleum. Environ. Sci. Technol. 46 (2), 619–627.

Caliskan, H., 2015. Novel approaches to exergy and economy based enhanced environmental analyses for energy systems. Energy Convers. Manag. 89, 156–161.

Chhipi-Shrestha, G., Hewage, K., Sadiq, R., 2017. Impacts of neighborhood densification on water-energy-carbon nexus: investigating water distribution and residential landscaping system. J. Clean. Prod. 156, 786–795.

Ciferno, J., 2008. Pulverized Coal Oxycombustion Power Plants Office of Systems. Analysis and Planning National Energy Technology Laboratory.

Davies, E.G.R., Kyle, P., Edmonds, J.A., 2013. An integrated assessment of global and regional water demands for electricity generation to 2095. Adv. Water Resour. 52, 296–313.

Davison, J., 2007. Performance and costs of power plants with capture and storage of CO2. Energy 32 (7), 1163–1176.

EIO-LCA, C.M.U.G.D.I., 2017. Economic Input-output Life Cycle Assessment (EIO-LCA), U.S. 2002 (428 Sectors) Purchaser Model Available from. www.eiolca.net. (Accessed 18 November 2017).

El-Dessouky, H.T., Ettouney, H.M., 2002. Fundamentals of Salt Water Desalination. Elsevier.

Evans, A., Strezov, V., Evans, T.J., 2009. Assessment of sustainability indicators for renewable energy technologies. Renew. Sustain. Energy Rev. 13 (5), 1082–1088.

Fang, D., Chen, B., 2018. Linkage analysis for water-carbon nexus in China. Appl. Energy 225, 682–695.

Freire-González, J., Font Vivanco, D., 2017. The influence of energy efficiency on other natural resources use: an input-output perspective. J. Clean. Prod. 162, 336–345.

Fthenakis, V., Kim, H.C., 2010. Life-cycle uses of water in U.S. electricity generation. Renew. Sustain. Energy Rev. 14 (7), 2039–2048.

Fu, Y., Liu, X., Yuan, Z., 2015. Life-cycle assessment of multi-crystalline photovoltaic (PV) systems in China. J. Clean. Prod. 86, 180–190.

Gagnon, L., Belanger, C., Uchiyama, Y., 2002. Life-cycle assessment of electricity generation options: the status of research in year 2001. Energy Pol. 30 (14), 1267–1278.

Gribov, B.G., Zinov'ev, K.V., 2003. Preparation of high-purity silicon for solar cells. Inorg. Mater. 39 (7), 653–662.

Gutowski, T.G., Sahni, S., Allwood, J.M., Ashby, M.F., Worrell, E., 2013. The energy required to produce materials: constraints on energy-intensity improvements, parameters of demand. Philos. Trans. A Math. Phys. Eng. Sci. 371 (1986), 20120003.

Hondo, H., 2005. Life cycle GHG emission analysis of power generation systems: Japanese case. Energy 30 (11–12), 2042–2056.

Hosseini, S.E., Barzegaravval, H., Ganjehkaviri, A., Wahid, M.A., Mohd Jaafar, M.N., 2017. Modelling and exergoeconomic-environmental analysis of combined cycle power generation system using flameless burner for steam generation. Energy Convers. Manag. 135, 362–372.

Hou, G., Sun, H., Jiang, Z., Pan, Z., Wang, Y., Zhang, X., Zhao, Y., Yao, Q., 2016. Life cycle assessment of grid-connected photovoltaic power generation from crystalline silicon solar modules in China. Appl. Energy 164, 882–890.

Ifaei, P., Ataei, A., Yoo, C., 2016a. Thermoeconomic and environmental analyses of a low water consumption combined steam power plant and refrigeration chillers-Part 2: thermoeconomic and environmental analysis. Energy Convers. Manag. 123, 625–642.

Ifaei, P., Karbassi, A., Jacome, G., Yoo, C., 2017a. A systematic approach of bottom-up assessment methodology for an optimal design of hybrid solar/wind energy resources – case study at middle east region. Energy Convers. Manag. 145, 138–157.

Ifaei, P., Karbassi, A., Lee, S., Yoo, C., 2017b. A renewable energies-assisted sustainable development plan for Iran using techno-econo-socio-environmental multivariate analysis and big data. Energy Convers. Manag. 153, 257–277.

Ifaei, P., Rashidi, J., Yoo, C., 2016b. Thermoeconomic and environmental analyses of a low water consumption combined steam power plant and refrigeration chillers - Part 1: energy and economic modelling and analysis. Energy Convers. Manag. 123, 610–624.

Janghorban Esfahani, I., Kang, Y.T., Yoo, C., 2014. A high efficient combined multi-effect evaporation–absorption heat pump and vapor-compression refrigeration part 1: energy and economic modeling and analysis. Energy 75, 312–326.

Jaramillo, P., Griffin, W.M., Matthews, H.S., 2007. Comparative life-cycle air emissions of coal, domestic natural gas, LNG, and SNG for electricity generation. Environ. Sci. Technol. 41 (17), 6290–6296.

Karan, E., Asadi, S., Mohtar, R., Baawain, M., 2018. Towards the optimization of sustainable food-energy-water systems: a stochastic approach. J. Clean. Prod. 171, 662–674.

Kılkış, Ş., Kılkış, B., 2017. Integrated circular economy and education model to address aspects of an energy-water-food nexus in a dairy facility and local contexts. J. Clean. Prod. 167, 1084–1098.

Kunanuntakij, K., Varabuntoonvit, V., Vorayos, N., Panjapornpon, C., Mungcharoen, T., 2017. Thailand Green GDP assessment based on environmentally extended input-output model. J. Clean. Prod. 167, 970–977.

Lee, S., Esfahani, I.J., Ifaei, P., Moya, W., Yoo, C., 2017. Thermo-environ-economic modeling and optimization of an integrated wastewater treatment plant with a combined heat and power generation system. Energy Convers. Manag. 142, 385–401.

Leung Pah Hang, M.Y., Martinez-Hernandez, E., Leach, M., Yang, A., 2016. Designing integrated local production systems: a study on the food-energy-water nexus. J. Clean. Prod. 135, 1065–1084.

Liu, Y., Qian, Y., Xiao, H., Yang, S., 2017. Techno-economic and environmental analysis of coal-based synthetic natural gas process in China. J. Clean. Prod. 166, 417–424.

Liu, Z., Geng, Y., Lindner, S., Zhao, H., Fujita, T., Guan, D., 2012. Embodied energy use in China's industrial sectors. Energy Pol. 49, 751–758.

Lora, E.E.S., Salomon, K.R., 2005. Estimate of ecological efficiency for thermal power plants in Brazil. Energy Convers. Manag. 46 (7–8), 1293–1303.

Macknick, J., Newmark, R., Heath, G., Hallett, K., 2011a. A Review of Operational Water Consumption and Withdrawal Factors for Electricity Generating Technologies. National Renewable Energy Laboratory (NREL).

Macknick, J., N, R., Heath, G., Hallett, K.C., 2011b. A Review of Operational Water Consumption and Withdrawal Factors for Electricity Generating Technologies. U.S. Department of Energy.

Meier, P.J., 2002. Life-cycle Assessment of Electricity Generation Systems and Applications for Climate Change Policy Analysis, Fusion Technology Indtitute. University of Wiscocsin.

Meier, P.J., Kulcinski, G.L., 2002. Life-cycle Energy Requirements and Greenhouse Gas Emissions for Building-integrated Photovoltaics. Fusion Technology Institute.

Meier, P.J., Wilson, P.P.H., Kulcinski, G.L., Denholm, P.L., 2005. US electric industry response to carbon constraint: a life-cycle assessment of supply side alternatives. Energy Pol. 33 (9), 1099–1108.

Meldrum, J., Nettles-Anderson, S., Heath, G., Macknick, J., 2013. Life cycle water use for electricity generation: a review and harmonization of literature estimates. Environ. Res. Lett. 8 (1), 015031.

Mi, Z.-F., Pan, S.-Y., Yu, H., Wei, Y.-M., 2015. Potential impacts of industrial structure on energy consumption and CO2 emission: a case study of Beijing. J. Clean. Prod. 103, 455–462.

Mintz, M., Saricks, C., Vyas, A., 2015. Coal-by-rail: a Business-as-usual Reference Case. Energy Systems Division, Argonne National Laboratory.

Moncada, J., Vural Gursel, I., Huijgen, W.J.J., Dijkstra, J.W., Ramírez, A., 2018. Techno-economic and ex-ante environmental assessment of C6 sugars production from spruce and corn. Comparison of organosolv and wet milling technologies. J. Clean. Prod. 170, 610–624.

Mostafaeipour, A., Sedaghat, A., Ghalishooyan, M., Dinpashoh, Y., Mirhosseini, M., Sefid, M., Pour-Rezaei, M., 2013. Evaluation of wind energy potential as a power generation source for electricity production in Binalood, Iran. Renew. Energy 52, 222–229.

Nafey, A.S., Sharaf, M.A., 2010. Combined solar organic Rankine cycle with reverse osmosis desalination process: energy, exergy, and cost evaluations. Renew. Energy 35 (11), 2571–2580.

Nair, S., George, B., Malano, H.M., Arora, M., Nawarathna, B., 2014. Water–energy–greenhouse gas nexus of urban water systems: review of concepts, state-of-art and methods. Resour. Conserv. Recycl. 89, 1–10.

Nitkiewicz, A., Sekret, R., 2014. Comparison of LCA results of low temperature heat plant using electric heat pump, absorption heat pump and gas-fired boiler. Energy Convers. Manag. 87, 647–652.

Onat, N.C., Kucukvar, M., Tatari, O., 2015. Conventional, hybrid, plug-in hybrid or electric vehicles? State-based comparative carbon and energy footprint analysis in the United States. Appl. Energy 150, 36–49.

Ou, Y., Zhai, H., Rubin, E.S., 2016. Life cycle water use of coal- and natural-gas-fired power plants with and without carbon capture and storage. Int. J. Greenh. Gas Control 44, 249–261.

Raluy, R.G., Serra, L., Uche, J., Valero, A., 2004. Life cycle assessment of water

production technologies - Part 2: reverse osmosis desalination versus the Ebro river water transfer (9 pp). Int. J. Life Cycle Assess. 10 (5), 346–354.
Rodríguez, R., Espada, J.J., Gallardo, M., Molina, R., López-Muñoz, M.J., 2018. Life cycle assessment and techno-economic evaluation of alternatives for the treatment of wastewater in a chrome-plating industry. J. Clean. Prod. 172, 2351–2362.
Safder, U., Ifaei, P., Yoo, C., 2018. Multi-objective optimization and flexibility analysis of a cogeneration system using thermorisk and thermoeconomic analyses. Energy Convers. Manag. 166, 602–636.
Shalaby, S.M., 2017. Reverse osmosis desalination powered by photovoltaic and solar Rankine cycle power systems: a review. Renew. Sustain. Energy Rev. 73, 789–797.
Shao, L., Guan, D., Wu, Z., Wang, P., Chen, G.Q., 2017. Multi-scale input-output analysis of consumption-based water resources: method and application. J. Clean. Prod. 164, 338–346.
Siddiqi, A., Anadon, L.D., 2011. The water–energy nexus in Middle East and North Africa. Energy Pol. 39 (8), 4529–4540.
Song, Q., Wang, Z., Wu, Y., Li, J., Yu, D., Duan, H., Yuan, W., 2018. Could urban electric public bus really reduce the GHG emissions: a case study in Macau? J. Clean. Prod. 172, 2133–2142.
Spath, P.L., Mann, M.K., Kerr, D.R., 1999. Life Cycle Assessment of Coal-fired Power Production. National Renewable Energy Laboratory (NREL).
Stokes, J.R., Horvath, A., 2009. Energy and air emission effects of water supply. Environ. Sci. Technol. 43 (8), 2680–2687.
Sui, X.W., Zhang, Y., Shao, S., Zhang, S.S., 2014. Exergetic life cycle assessment of cement production process with waste heat power generation. Energy Convers. Manag. 88, 684–692.
Thiede, S., Schönemann, M., Kurle, D., Herrmann, C., 2016. Multi-level simulation in manufacturing companies: the water-energy nexus case. J. Clean. Prod. 139, 1118–1127.
Turconi, R., Boldrin, A., Astrup, T., 2013. Life cycle assessment (LCA) of electricity generation technologies: overview, comparability and limitations. Renew. Sustain. Energy Rev. 28, 555–565.
U.S.EPA, 2016. Inventory of U.S. Greenhouse Gas Emissions and Sinks: 1990 - 2014.
Voorspools, K.R., Brouwers, E.A., D'haeseleer, W.D., 2000. Energy content and indirect greenhouse gas emissions embedded in 'emission-free' power plants: results for the Low Countries. Appl. Energy 67 (3), 307–330.
White, S.W., Kulcinski, G.L., 2000. Birth to death analysis of the energy payback ratio and CO2 gas emission rates from coal, fission, wind, and DT-fusion electrical power plants. Fusion Eng. Des. 48 (3–4), 473–481.
Wiedmann, T.O., Suh, S., Feng, K., Lenzen, M., Acquaye, A., Scott, K., Barrett, J.R., 2011. Application of hybrid life cycle approaches to emerging energy technologies–the case of wind power in the UK. Environ. Sci. Technol. 45 (13), 5900–5907.
Wu, Y., Zhang, L., 2017. Can the development of electric vehicles reduce the emission of air pollutants and greenhouse gases in developing countries? Transport. Res. Part D Transport Environ. 51, 129–145.
Yang, D., Liu, B., Ma, W., Guo, Q., Li, F., Yang, D., 2017. Sectoral energy-carbon nexus and low-carbon policy alternatives: a case study of Ningbo, China. J. Clean. Prod. 156, 480–490.
Yang, J., Chen, B., 2016. Energy–water nexus of wind power generation systems. Appl. Energy 169, 1–13.

Nomenclature

W_{turb}: steam turbine's power
$\dot{m}$: mass flowrate
h: specific enthalpy
W_{pump}: pump's power consumption
η_{pump}: pump's isentropic efficiency
P_{in}: pressure of inflow
P_{out}: pressure of outflow
v: specific volume
c_p: specific heat capacity
ε_{HEX}: heat exchanger effectiveness
$\Delta T_{\min}$: temperature difference between the inflow and outflows
SgV: sign variable
W_{NRES}: direct power produced by the NRES
W_{op}: operational power
W_{up}: indirect power at upstream stage
Q_{in}: furnace's thermal power
SRR: salt rejection ratio
RR: membrane's recovery ratio
X: salt concentration
f: feedwater
b: brine
d: distillate
$\Delta\Pi_{av}$: the average osmotic pressure
P_d: the pressure of the distillate
TCF: temperature correction factor
FF: fouling factor
N_e: number of elements
N_v: number of vessels in each stage
A_{memb}: membrane active surface
K_w: pure water permeability
T_f: feedwater temperature
X_b: brine salt concentration
W_{RO}: required power in the RO pump
SPC: specific power consumption
ρ: density
Y_{PV}: power output of the PV module under STC
f_{PV}: derating factor
$G_{T,STC}$: solar radiation under STC
α_P: temperature coefficient
T_C: PV cell's temperature
T_a: ambient temperature
$T_{C,NOCT}$: nominal cell temperature
$\eta_{mp,STC}$: maximum efficiency under the STC
τ: solar transmittance
ν: solar absorbance
G_T: solar radiation on the panel
G_g: global radiation
G_d: diffuse radiation on a flat horizontal surface
R_b: ratio of the average direct beam on a tilted surface to a horizontal one
g_a: ground albedo
β: tilt angle between the panel and the ground
η_i: the efficiency of the inverter
F_{total}: total loss factor
W_{theory}: theoretical power
ρ_{hub}: wind density
V_{hub}: wind speed at the hub height of the turbine
A: area swept by the turbine rotor
C_P: the maximum theoretical efficiency of the turbine
P : air pressure
R_d: global gas constant
T : average air temperature
V_{anem}: wind speed at the anemometer height
H_b: heating rate of the boiler
ΔT_{OFWH}: difference between saturated inflow and outflow temperature of the OFWH
η_{turb}: the turbine's isentropic efficiency
$CC_{ref.HEX}$: the PEC of the referenced heat exchanger
N_{labor}: number of labors
lf: loading factor
lt_{memb}: the membrane's life time
TAC: the total annualized cost
ACC: annual capital cost
AOC: annual operation cost
CRF: amortization factor
IM: interactions matrix
$A_{ref.HEX}$: the area of the referenced heat exchanger
Q_{HEX}: the actual heat transfer rate of a heat exchanger
TD: the temperature difference between the cooled water and inlet air wet bulb temperature in the NDWCT
CI: chemical engineering plant cost index
DCC: direct capital cost
CC_{swip}: seawater intake capital cost
CC_{equip}: the cost of equipment
CC_{memb}: the unitary membrane base cost
CC_{site}: the site development cost
CC_{instal}: the installation cost
ICC: indirect capital cost
TCC_{RO}: total capital costs of the RO
CC_{civil}: summation of the civil costs
CC_{eng}: engineering and supervision costs
CC_{PEC}: purchased equipment costs
CC_{conti}: contingency costs
OM_{labor}: summation of the labor costs
OM_{power}: power costs
OM_{power}: chemical costs
OM_{memb}: membrane costs
ir: interest rate
lc: life cycle
rm: required material
ei: energy intensity
wi: water intensity
DC: direct carbon
cpc: combustion pollutant coefficient
mf: multiplication factor
η_{fur}: thermal efficiency of the furnace
IC: indirect carbon
RP: released portion
$\dot{m}_{fuel}$: required fuel
LHV_{fuel}: lower heating value of the fuel
mf: methane to carbon dioxide coefficient
W_F: required water for fuel
E_F: required energy for fuel

E_E: required energy in energy sector
E_W: required energy in water sector
E_C: required energy in carbon sector
W_E: required water in energy sector
W_W: required water in water sector
W_C: required water in carbon sector
C_E: emitted carbon in energy sector
C_W: emitted carbon in water sector
C_C: emitted carbon in carbon sector
i: number of elements in a pressure vessel
j: number of vessels in a stage
k: Number of parallel stages in a module
X: a product's quantity
l: iteration counter
EcCP: economic cost of products
EnCP: environmental cost of products
CEECP: combined economic-environmental cost of products
WEF: water-energy factor
WPC: environmental water penalty cost
CPC: carbon penalty cost
Y: output variable
Y_{max}: maximum quantity of the response in the control range

Abbreviations

WEC: water-energy-carbon
PCA: process chain analysis
LCA: life cycle assessment
LCIA: life cycle inventory analysis
HRES: hybrid renewable energy system
NRES: non-renewable energy system
RO: reverse osmosis
PV: solar photovoltaic
WT: wind turbine
CV: control valve
OFWH: open feedwater heater
SHX: solution heat exchanger
HEX: heat exchanger
STC: standard test conditions
EIO: economic input/output
GDP: gross domestic product
GGDP: green gross domestic product